Benzo[*a*]pyrene Diol Epoxide Forms Covalent Adducts with Deoxycytidylic Acid by Alkylation at Both Exocyclic Amino N^4 and Ring Imino N-3 Positions

Alan R. Wolfe,* Timothy J. Smith,† and Thomas Meehan‡

Department of Biopharmaceutical Sciences, University of California, San Francisco, California 94143-0446

Received February 10, 2003

The carcinogen 7r,8t-dihydroxy-9t,10t-epoxy-7,8,9,10-tetrahydrobenzo[*a*]pyrene (*anti*-BPDE) alkylates DNA at dGuo, dAdo, and dCyd. dCyd adducts, formed in small amounts, elute near the more abundant dGuo adducts. We isolated the dCyd adducts formed with dCMP. Each BPDE enantiomer forms three major adducts with dCMP, two cis and one trans. The trans adduct and one of the cis adducts form by alkylation at exocyclic N^4, while the second cis adduct is a dUrd adduct formed by alkylation at ring N-3 followed by deamination. Epoxide ring-opening geometries were assigned on the basis of halide and temperature effects on adduct yield, the sign of the major CD band, and benzo ring proton NMR coupling constants. One of each set of cis adducts is fluorescent (FL), and the other is nonfluorescent (NF). The trans and FL cis adducts have fluorescence quantum yields 40−50% of that of the BPDE hydrolysis product. The long wavelength UV maxima of the FL and NF cis adducts are red-shifted 1 and 3 nm relative to the trans adduct. ^{1}H NMR deuterium exchange experiments indicate that in the trans and FL cis adducts N^4−H is coupled to C10−H. Adduct formation experiments with methyl-protected Cyd derivatives show that NF cis adducts result from alkylation at N-3. MS results, pK_a measurements, and dUrd alkylation experiments indicate that the N-3 dCyd adducts spontaneously deaminate to dUrd adducts. NMR coupling constants show that in the NF cis adduct the C7 and C8 substituents are quasi equatorial and the C9 substituent is quasi axial, unlike in other cis BPDE adducts. ^{1}H NOESY spectra of the (−)-BPDE NF cis adduct reveal that it exists in two conformers. Molecular modeling shows that the conformers result from two low-energy conformations of very similar energies with the pyrimidine in opposite orientations, separated by significant barriers to rotation of the uracil moiety.

Introduction

The PAH[1] BaP is a ubiquitous environmental contaminant and a mammalian carcinogen. BaP is oxidized to four stereoisomeric diol epoxides, which have been recognized as ultimate carcinogens. The most mutagenic and carcinogenic of these is (+)-*anti*-BPDE. *anti*-BPDE forms a number of stable and unstable covalent adducts with DNA bases both in vitro and in vivo. Reaction with DNA also catalyzes the hydrolysis of *anti*-BPDE, leading to the formation of stereoisomeric 7,8,9,10-tetrahydro-7,8,9,10-tetrahydroxy derivatives (*cis*- and *trans*-BPT). Normally, a small fraction (≤10%) of the BPDE added to an aqueous solution of DNA forms covalent adducts, while the remainder is converted to the tetrol hydrolysis products (*1*).

The major stable adduct formed by reaction of racemic *anti*-BPDE with DNA results from nucleophilic attack of the exocyclic N^2 position of guanine on the C-10 position of (+)-*anti*-BPDE, with trans opening of the epoxide ring (*1*−*4*). Because of the possibility of both cis and trans addition of the nucleophile, *anti*-BPDE forms three other covalent adducts with this alkylation target. *anti*-BPDE similarly forms four DNA adducts with the exocyclic N^6 amino group of adenine. Adducts with N^2 of dGuo generally constitute about 90% of the stable DNA alkylation products formed by reaction with *anti*-BPDE, while dAdo adducts make up most of the balance (*3*, *5*).

A considerable amount of work has been carried out on the properties and biological effects of the major adducts formed by *anti*-BPDE. However, in addition to epoxides, PAH carcinogens form radical cations (*6*, *7*) and quinones (*8*), both of which can alkylate DNA; the latter may also exert biological activity via redox cycling. Thus, at least three pathways could contribute to carcinogenesis and promotion by PAHs.

We have demonstrated that halide ions catalyze the alkylation of DNA by *anti*-BPDE and that halohydrins are intermediates in this process (*9*−*13*). Chlorohydrins are formed at physiological concentrations of salt and generate the same exocyclic amino group adducts as epoxides. However, alkylation by chlorohydrins in vitro favors cis adduct formation and increases overall adduct

* To whom correspondence should be addressed. Tel: (415)476-2307. Fax: (415)476-0688. E-mail: alwolfe@itsa.ucsf.edu.

† Present address: Lion Bioscience Research Inc., 141 Portland St., Cambridge, MA 02139.

‡ Present address: Deep Sea DNA Corp., 1160 Brickyard Cove Rd. B-21, Point Richmond, CA 94801.

[1] Abbreviations: PAH, polycyclic aromatic hydrocarbon; BaP, benzo[*a*]pyrene; (+)-*anti*-BPDE, 7*R*,8*S*-dihydroxy-9*S*,10*R*-epoxy-7,8,9,10-tetrahydrobenzo[*a*]pyrene; (−)-*anti*-BPDE, 7*S*,8*R*-dihydroxy-9*R*,10*S*-epoxy-7,8,9,10-tetrahydrobenzo[*a*]pyrene; *trans*-BPT, racemic 7r,8t,-9t,10c-tetrahydroxy-7,8,9,10-tetrahydrobenzo[*a*]pyrene; *cis*-BPT, racemic 7r,8t,9t,10t-tetrahydroxy-7,8,9,10-tetrahydrobenzo[*a*]pyrene; FL, fluorescent; NF, nonfluorescent; WF, weakly fluorescent; RA, relative abundance; COSY, correlation NMR spectroscopy; NOESY, nuclear Overhauser effect NMR spectroscopy.

10.1021/tx0340201 CCC: $27.50
Published on Web 03/03/2004

yield. When applied to rodent skin ex vivo, the chlorohydrin of *anti*-BPDE produces DNA adducts whose cis proportion is 50% or greater (*14*) (in this situation, adduct yield is low owing to the instability of the chlorohydrin coupled with the requirement for diffusion to the alkylation target). Alkylation of DNA by BPDE chlorohydrin formed in vivo is suggested by the larger than typical proportion of cis adducts (∼16%) generated by BPDE applied to cat salivary cell cultures.[2] Secretory epithelial cells such as these have been found to have internal chloride concentrations of 40−90 mM (*15, 16*), while values of 5−15 mM are typical of nonepithelial cells (nonsecretory epithelial cells are intermediate).

Because of the similarity of the target, some alkylation of DNA by BPDE at the exocyclic amino group (N^4) of cytosine would also be expected. Some evidence indicative of dCyd alkylation by BPDE has been reported (*17*−*21*), but definitive dCyd adduct structural data were not obtained. A trans N^4 adduct, whose abundance was 2% of total products derived from reaction of (−)-*anti*-BPDE with denatured DNA, was tentatively identified on the basis of MS and CD (*21*); a trace of the putative corresponding (+)-*anti*-BPDE adduct was also observed. Mass spectral evidence has shown that *anti*-BPDE forms N^4-cytidine adducts in RNA (*22*), but the stereochemistry of these adducts was not identified. Confirming the formation of dCyd adducts is made difficult by the similarity of their reverse phase HPLC retentions to those of the more abundant dGuo adducts (*17, 21*). In the cases of dibenz[*a*,*j*]anthracene 3,4-diol-1,2-epoxide (*23, 24*) and benz[*a*]anthracene 3,4-diol-1,2-epoxide (*25*), dCyd adducts make up 12−14 and 7% of total DNA adducts, respectively, and their structures have been determined. In both cases, the (*S*,*R*,*R*,*S*) [(−)-anti] isomer of the epoxide forms a trans N^4 dCyd adduct. The (*S*,*R*,*R*,*S*) isomer [in this case, (+)-anti] of benzo[*c*]-phenanthrene diol epoxide has been found to generate a dCyd adduct comprising 11% of total DNA adducts (*26, 27*), but its structure was not established. There have been several reports of the formation of unstable, alkali sensitive dCyd adducts in DNA modified by *anti*-BPDE (*28*) or by anti and syn bay region diol epoxides of benzo-[*c*]phenanthrene (*29*). In the former case, alkali labile lesions at dCyd were estimated to comprise 5% of total BPDE adducts, and N-3 or O^2 alkylation sites were suggested as possibilities.

The relationship between DNA alkylation and tumorigenesis is not simple. An adduct's stereochemistry or alkylation site can influence its relative contribution in ways that are not fully understood. Cis adducts of BPDE and benzo[*c*]phenanthrene 3,4-diol 1,2-epoxide tend to be more mutagenic than the corresponding trans adducts on a single-stranded vector in *Escherichia coli* (a system in which the influence of repair should be minimal) (*30*). A number of observations have been made implying a correlation between a PAH diol epoxide's extent of reaction with dAdo, normally a minor alkylation target, and its tumorigenicity, suggesting that dAdo adducts may tend to be more tumorigenic than dGuo adducts (*27, 31*). In the case of adducts of (+)-*anti*-BPDE, an example has been found in mammalian cells of a situation where the dGuo adducts are excised from the transcribed DNA strand with much greater efficiency than dAdo adducts (*32*). Repair mechanisms may tend to be less efficient for less common types of adducts, with the consequence that minor adducts could play a role in tumor initiation greater than their abundance might suggest. Whether this is true of BPDE−dCyd adducts is not yet known.

We examined adduct formation between dCMP and *anti*-BPDE to obtain structural data and chromatographic standards that could be used to investigate the formation and occurrence of stable dCyd adducts in DNA. (Unstable or alkali labile adducts would have been lost in our isolation procedure and are thus outside the scope of our study.) The monophosphate was used as a target because it permits elimination (via solvent extraction) of hydrolysis products and impurities present in the BPDE preparation. In this report, we demonstrate that each enantiomer of *anti*-BPDE alkylates dCMP with the formation of three principal adducts. Two of three are cis and trans N^4 deoxycytosine adducts, while the third, and most abundant, is an unusual NF cis deoxyuridine adduct formed by alkylation of pyrimidine ring nitrogen N-3 followed by deamination. Identification of adduct stereochemistry was facilitated by observing changes in adduct levels in response to halides, illustrating the utility of the halohydrin alkylation pathway in the characterization of epoxide−DNA adducts. This is the first report of a bay region dihydrodiol epoxide generating an adduct with a pyrimidine ring nitrogen.

Experimental Procedures

Caution: *anti-BPDE is carcinogenic and should be handled carefully. Glassware contaminated with anti-BPDE was soaked in a monobasic sodium phosphate solution overnight prior to cleanup.*

Chemicals. Resolved *anti*-BPDE enantiomers were synthesized as described previously (*33*). Tritium-labeled *anti*-BPDE enantiomers were obtained from the NCI Chemical Carcinogen Reference Standard Repository.

Instruments. CD spectra were taken on a JASCO J-500A Spectropolarimeter. Absorption spectra were taken with a Cary 3E spectrophotometer. Proton NMR spectra of peracetylated adducts in acetone-d_6 or of nonacetylated NF cis dCyd adduct in DMSO-d_6 were taken at 600 MHz with a Varian INOVA 600 spectrometer using a 3 mm probe. A TMS standard was used. The temperature was generally 25 °C for samples in acetone-d_6 and 30 °C for samples in DMSO-d_6 (one spectrum using DMSO-d_6 was obtained at 80 °C). Proton resonances were assigned on the basis of coupling constants and two-dimensional homonuclear COSY spectra in the cases of the trans dCyd and FL cis dCyd adducts and additionally by using two-dimensional NOESY spectra in the case of the NF cis adduct, using mixing times of 400 (in DMSO-d_6) or 600 ms (in acetone-d_6). In the NOESY spectra, cross-peaks due to chemical exchange are distinguishable from those due to the nuclear Overhauser effect by sign. Mass spectrometry was performed using a SCIEX API 3000 instrument for electrospray spectra and a Micromass VG70 for electron impact spectra.

Preparation of BPDE-Modified Polyribonucleotides. Adducts were generated between resolved enantiomers of *anti*-[^{3}H]BPDE and ribonucleotide homopolymers in solutions containing 10 mM, pH 7.5, sodium phosphate buffer, 3% (v/v) acetone, 12 μM BPDE, and 1 mg/mL of poly(A), poly(C), or poly(G). The reaction proceeded overnight at room temperature. The solutions were brought to 100 mM NaCl by addition of 4 M NaCl, and each sample was extracted five times with 2 mL of buffer-saturated ethyl acetate. The samples were then dialyzed eight times in 900 mL of 2 mM, pH 7.5, sodium phosphate buffer containing 1 mM EDTA and 100 mM NaCl, using 2000 MW cutoff Spectrapor dialysis tubing, for a total of 106 h of dialysis.

[2] NEF36.Sg cells (American Type Culture Collection No. CRL-6176). Wolfe, A. R., Wang, I. X., and Meehan, T. Unpublished results.

(The NaCl and EDTA serve to remove Mg^{2+}, an RNase cofactor, thus inhibiting any RNases present.)

Following dialysis, the modified polyribonucleotides were precipitated with 2.5 volumes of cold ethanol, kept at −20 °C for 2 h, and centrifuged for 10 min at 13 000*g*. The supernatant solutions were frozen at −80 °C, thawed, and centrifuged again. The combined pellets for each sample were dried and dissolved in water at a concentration of 1 mg/mL RNA. KOH was added to give a final concentration of 0.3 M, and the samples were boiled for 15 min to hydrolyze the RNA. Then, the samples were treated with alkaline phosphatase as described below (using HCl to adjust the pH of the samples to 10). Purification of the adducts with C_{18} Sep-Paks was also as described below.

Preparation of dCMP Adducts. Adducts of dCMP were generally prepared in solutions containing 100 μM (+)- or (−)-*anti*-BPDE, 5% THF, 5 mM (pH 7.6) HEPES, 50 mM dCMP, and varying amounts of NaCl and KBr. The reaction mixtures were incubated at 0, 23, or 37 °C. Scaled up reactions for preparative purposes were initiated with 30 mM dCMP, 30 mM KBr, and 500 μM *anti*-BPDE (because this concentration of BPDE greatly exceeds its solubility in the solution used, the latter was added in two portions separated by several hours). The reactions were allowed to proceed for several hours in the dark or for 20 h in the case of preparative scale reactions.

KOH (final concentration 25 mM) was then added to the reaction mixtures to raise the pH to 11.9, to put two negative charges on the phosphomonoesters. The samples were then extracted seven times with water-saturated 1-butanol, followed by four times with 2 mL of diethyl ether, to remove most of the BPDE hydrolysis products (*trans*- and *cis*-BPT), as well as any impurities from the BPDE sample. (Samples of resolved *anti*-BPDE enantiomers are likely to be less pure than those of racemic BPDE, because enantiomerically pure BPDE does not readily crystallize.) Traces of solvent remaining in the aqueous phase were removed with a stream of air.

The samples were then brought to 25 mM glycine, 0.3 mM $ZnCl_2$, and 0.5 mM $MgCl_2$. KOH was added to bring the pH to 10.0. Alkaline phosphatase (10 U/μmol nucleotide) was added, followed by additional KOH to bring the pH back to 9.8. After 6 h of incubation at 37 °C, an additional 5 U of alkaline phosphatase/μmol was added, plus additional KOH to maintain pH at 9.8. Incubation was continued at 37 °C for six more hours and then at room temperature overnight.

Unmodified nucleosides were eliminated by C_{18} Sep-Pak chromatography. Samples were diluted 1:5 with H_2O and loaded onto a Sep-Pak cartridge (Waters Corp., Milford, MA), which was washed with 20 mL of 10% methanol:water to elute unmodified dCyd, followed by 2.5 mL of methanol to elute the adducts. Adduct samples were stored in methanol at −20 °C. Prior to HPLC, the samples were evaporated under reduced pressure, redissolved in 42% methanol:water, and filtered using 0.2 μm Nylon-66 membranes. (Some alkylation reactions were also performed with dCyd by the same procedure as for dCMP, except omitting the organic extraction and alkaline phosphatase digestion steps.) Adducts were per-O-acetylated by reacting overnight in 5:2 pyridine:acetic anhydride.

Singly primed numbers (1′−5′) designate protons on the deoxyribose moiety of adducts, and doubly primed numbers (5″−6″) designate protons on the pyrimidine moiety.

(+) FL cis dCyd Adduct. UV λ_{max} [methanol]: 245.0, 278.75, 344.0 nm. CD [methanol]: +, −, −.

(+)-trans dCyd Adduct. UV λ_{max} [methanol]: 245.75, 279.25, 343.25 nm. CD [methanol]: −, +, +.

(+) NF cis dCyd Adduct. UV λ_{max} [methanol]: 246.5, 279.0, 346.25 nm. CD [methanol]: +, −, +.

(−)-trans dCyd Adduct. UV λ_{max} [methanol]: 246.0, 279.25, 343.25 nm. CD [methanol]: +, −, −. ^{1}H NMR of peracetylated adduct (acetone-d_6): δ 8.347 (d, 1, H_1 or H_3, J = 7.55 Hz), 8.334 (d, 1, H_1 or H_3, J = 7.55 Hz), 8.296 (d, 1, H_{11} or H_{12}, J = 9.3 Hz), 8.216 (d, 1, H_4 or H_5, J = 9.0 Hz), 8.202 (d, 1, H_4 or H_5, J = 8.2 Hz), 8.178 (s, 1, H_6), 8.176 (d, 1, H_{11} or H_{12}, J = 8.9 Hz), 8.115 (t, 1, H_2, J = 7.56, 7.69 Hz), 7.81 (d, 1, $H_{6''}$, J = 7.6 Hz), 7.63 (d, 1, N^4-H, exchanges with D_2O), 6.78 (d, 1, H_7, J = 9.5 Hz), 6.44 (dd, 1, H_{10}, J = 2.6, 7.9 Hz, after D_2O exchange reduces to d, J = 2.7 Hz), 6.37 (dd, 1, $H_{1'}$, J = 5.8, 8.1 Hz), 5.98 (dd, 1, H_9, J < 4 Hz), 5.88 (d, 1, $H_{5''}$, J = 7.0 Hz), 5.73 (dd, 1, H_8, J = 1.7, 9.9 Hz), 5.32 (dt, 1, $H_{3'}$, J = 2.0, 6.4 Hz), 4.32, (m, 1, $H_{4'}$), 3.32 + 3.07 (m, 2, $H_{5'}$), 2.58 + 2.40 (m, 2, $H_{2'}$). MS: positive mode electrospray of the per-O-acetylated adduct ($C_{39}H_{37}N_3O_{12}$, monoisotopic mass 739.2377) gave the major peak in the 460−850 *m*/*z* range (with % RA based only on peaks in this range) at 740.4 (100% RA, M + H^+), with all other peaks ≤24% RA. High-resolution EI-MS of the per-O-acetylated adduct gave the three largest peaks in the 500−850 *m*/*z* range at 679.214442 (2.1% RA, consistent with M − CH_3COOH, with expected *m*/*z* 679.216595 for a 3.2 ppm discrepancy), 619.196161 (7.1% RA, consistent with M − 2 CH_3COOH, with expected *m*/*z* 619.195465 for a −1.1 ppm discrepancy), and 561.189583 (2.1% RA; not identified).

(−) NF cis dCyd (dUrd) Adduct. UV λ_{max} [methanol]: 246.75, 279.0, 346.25 nm. CD [methanol]: −, +, −. ^{1}H NMR of peracetylated adduct (acetone-d_6) major conformer: δ 8.292 (d, 1, H_3, J = 7.33 Hz), 8.256 (d, 1, H_1, J = 7.69 Hz), 8.196 (s, 1, H_6), 8.176 (d, 1, H_4, J = 5.13 Hz), 8.150 (d, 1, H_5, J = 5.49 Hz), 8.148 (d, 1, H_{12}, J = 9.15 Hz), 8.056 (t, 1, H_2, J = 7.69 Hz), 7.862 (d, 1, H_{11}, J = 9.53 Hz), 7.786 (d, 1, $H_{6''}$, J = 8.06 Hz), 7.520 (d, 1, H_{10}, J = 6.96 Hz), 7.046 (d, 1, H_7, J = 10.25 Hz), 6.160 (dd, 1, H_9, J = 3.29, 6.96 Hz), 5.992 (d, 1, $H_{5''}$, J = 8.06 Hz), 5.878 (dd, 1, $H_{1'}$, J = 5.86, 8.43 Hz), 5.517 (dd, 1, H_8, J = 3.29, 10.25 Hz), 5.055 (dt, 1, $H_{3'}$, J = 2.20, 2.56, 6.59 Hz), 4.133 (m, 1, $H_{4'}$, J = 2.93, 3.66, 4.03, 6.59 Hz [partial list]), 3.309 + 3.089 (m, 2, $H_{5'}$), 2.09 + 1.90 (m, 2, $H_{2'}$). Minor conformer: δ 8.284 (d, 1, H_3), 8.244 (d, 1, H_1), 8.176 (d, 1, H_4), 8.165 (s, 1, H_6), 8.148 (d, 1, H_{12}), 8.150 (d, 1, H_5), 8.043 (t, 1, H_2, J = 8.42 Hz), 7.945 (d, 1, H_{11}, J = 9.53 Hz), 7.736 (d, 1, $H_{6''}$, J = 8.06 Hz), 7.390 (d, 1, H_{10}, J = 6.22 Hz), 7.064 (d, 1, H_7, J = 11.36 Hz), 6.483 (dd, 1, $H_{1'}$, J = 5.49, 5.86, 7.69, 8.06 Hz), 6.176 (dd, 1, H_9, J = 2.93, 3.30, 6.22, 6.59 Hz), 5.546 (dd, 1, H_8, J = 2.93, 3.30, 9.89, 10.26 Hz), 5.380 (d, 1, $H_{5''}$, J = 8.05 Hz), 5.338 (dt, 1, $H_{3'}$, J = 2.20, 2.57, 6.59 Hz), 4.405 (m, 1, $H_{4'}$, J = 2.93, 3.66, 4.40, 6.59 Hz [partial list]), 3.903 + 3.757 (m, 2, $H_{5'}$), 2.65 + 2.43 (m, 2, $H_{2'}$). ^{1}H NMR of nonacetylated adduct (DMSO-d_6) [Note that the putative methine and $H_{5'}$ resonances in the COSY and NOESY spectra of the nonacetylated (−) NF cis adduct in DMSO exhibited a number of puzzling features and are not shown; only those resonances that could be assigned in a straightforward manner are listed.] major conformer: δ 8.493 (s, 1, H_6), 8.248 (d, 1, H_3, J = 7.69 Hz), 8.198 (d, 1, H_1, J = 7.51 Hz), 8.170 (d, 1, H_5, J = 8.98 Hz), 8.114 (d, 1, H_4, J = 9.34 Hz), 8.082 (d, 1, H_{12}, J = 9.34 Hz), 8.011 (t, 1, H_2, J = 7.51, 7.69 Hz), 7.920 (d, 1, $H_{6''}$, J = 8.06 Hz), 7.714 (d, 1, H_{11}, J = 9.515 Hz), 5.98 (d, 1, $H_{5''}$, J = 8.06 Hz), 5.67 (t, 1, $H_{1'}$, J = 6.41, 6.59 Hz), 4.91 (d, 1, $H_{4'}$, J = 4.03 Hz), 3.99 (1, $H_{3'}$), 1.51 + 1.56 (m, 2, $H_{2'}$). Minor conformer: δ 8.463 (s, 1, H_6), 8.248 (d, 1, H_3, J = 7.69 Hz), 8.198 (d, 1, H_1, J = 7.51 Hz), ∼8.16 (d, 1, H_5), 8.106 (d, 1, H_{12}, J = 9.34 Hz), ∼8.1 (1, H_4), 8.011 (t, 1, H_2, J = 7.51, 7.69 Hz), 7.862 (d, 1, $H_{6''}$, J = 7.87 Hz), ∼7.74 (d, H_{11}), 6.47 (t, 1, $H_{1'}$, J = 6.22, 6.96 Hz), 5.34 (d, 1, $H_{4'}$, J = 4.03 Hz), 5.29 (d, 1, $H_{5''}$, J = 8.06 Hz), 4.29 (1, $H_{3'}$), 2.20 + 2.26 (m, 2, $H_{2'}$). MS: positive mode electrospray of the nonacetylated adduct ($C_{29}H_{26}N_2O_8$, monoisotopic mass 530.1689) gave major peaks in the 500−650 *m*/*z* range (with % RA based only on peaks in this range) at 569.2 (26% RA, M + K^+), 553.2 (100% RA, M + Na^+), 531.2 (24% RA, M^+), 527.2 (45% RA, not identified), with all other peaks ≤12% RA. High-resolution EI-MS of the per-O-acetylated adduct ($C_{39}H_{36}N_2O_{13}$, monoisotopic mass 740.2217) gave the two largest peaks in the 470−850 *m*/*z* range at 680.209328 (2.6% RA, consistent with M − CH_3COOH, with expected *m*/*z* 680.200610 for a −12.8 ppm discrepancy) and at 620.180877 (9.5% RA, consistent with M − 2 CH_3COOH, with expected *m*/*z* 620.179481 for a −2.3 ppm discrepancy).

(−) FL cis dCyd Adduct. UV λ_{max} [methanol]: 245.25, 279.0, 344.25 nm. CD [methanol]: −, +, +. ^{1}H NMR of peracetylated adduct (acetone-d_6): δ 8.338 (d, 2, H_1+ H_3, J = 7.69 Hz), 8.275

(d, 1, H_4 or H_5, J = 9.25 Hz), 8.267 (s, 1, H_6), 8.250 (d, 1, H_4 or H_5, J = 9.34 Hz), 8.218 (d, 1, H_{11} or H_{12}, J = 8.97 Hz), 8.159 (d, 1, H_{11} or H_{12}, J = 8.97 Hz), 8.119 (t, 1, H_2, J = 7.60 Hz), 7.734 (d, 1, $H_{6''}$, J = 7.42 Hz), 6.952 (d, 1, N^4-H, J = 9.06 Hz, exchanges with D_2O), 6.909 (dd, 1, H_{10}, J = 4.94, 9.06 Hz, after D_2O exchange reduces to d, J = 4.95 Hz), 6.620 (d, 1, H_7, J = 4.12 Hz), 6.416 (dd, 1, $H_{1'}$, J = 5.68, 8.42 Hz), 5.968 (dd, 1, H_9, J = 2.20, 2.29, 4.86, 4.95 Hz), 5.911 (d, 1, $H_{5''}$, J = 7.41 Hz), 5.643 (dd, 1, H_8, J = 2.29, 4.03 Hz), 5.303 (dt, 1, $H_{3'}$, J = 2.29, 2.38, 6.59 Hz), 4.32 (m, 1, $H_{4'}$), 3.31 + 3.08 (m, 2, $H_{5'}$), 2.54 + 2.36 (m, 2, $H_{2'}$). MS: positive mode electrospray of the per-O-acetylated adduct ($C_{39}H_{37}N_3O_{12}$, monoisotopic mass 739.2377) gave the major peak in the 420−890 *m*/*z* range (with % RA based only on peaks in this range) at 740.2 (100% RA, M + H^+), with all other peaks ≤5% RA. High-resolution EI-MS of the per-O-acetylated adduct gave the largest peak in the 480−760 *m*/*z* range at 619.193186 (2.1% RA, consistent with M − 2 CH_3COOH, with expected *m*/*z* 619.195465 for a 3.7 ppm discrepancy).

Preparation of Cytidine Adducts. Adducts of cytidine, 2′-O-methylcytidine, or 3-methylcytidine were prepared using 2 mL samples of solutions containing 10−20 mM nucleoside, 30 mM KBr, and 3.75 mM (pH 7.6) HEPES buffer. If necessary, NaOH was added to bring the sample pH to 7.6.

A 1.35 μmol sample of (+)-*anti*-BPDE was purified by HPLC using a 0.39 cm × 30 cm Waters Prep Nova-Pak HR Silica column with a mobile phase of 35% ethyl acetate:hexane (the ethyl acetate component contained 0.5% ethanol to reduce silica reactivity) and a flow rate of 1.0 mL/min. Detection was by absorbance at 365 nm (above the 345 nm λ_{max} to reduce intensity). The BPDE peak near 20 min was collected and divided into three equal portions (450 μL), which were added to the three samples. The organic layers were removed from the samples under reduced pressure in a rotary evaporator. An aliquot of THF (0.10 mL) was then added to bring each sample to 5% THF. The samples were vortexed and allowed to react overnight at room temperature. Samples were then diluted with water to 20 mL and subjected to C_{18} cartridge chromatography as described above to remove unreacted nucleoside. CMP adducts of (+)-*anti*-BPDE were prepared by the procedure described for dCMP adducts.

(+) Cyd Adduct 1 (Putative N^4 cis, Observed Only in Adducts from CMP). UV λ_{max} [methanol]: 245.25, 278.75, 344.25 nm. Fluorescence/absorbance ratio = 35 (normalized to 100 for BPT).

(+) Cyd Adduct 2 (Putative N^4 trans). UV λ_{max} [methanol]: 246.25, 278.5, 343.25 nm. Fluorescence/absorbance ratio = 19.

(+) Cyd Adduct 3 (Putative N-3 cis). UV λ_{max} [methanol]: 246.75, 279.0, 346.25 nm. Fluorescence/absorbance ratio ≈ 0.

(+) 3-MethylCyd Adduct (Putative N^4 trans). UV λ_{max} [methanol]: 245.75, 277.5, 342.0 nm. Fluorescence/absorbance ratio = 20.

(+) 2′-O-MeCyd Adduct 1 (Putative N^4 trans). UV λ_{max} [methanol]: 245.5, 277.75, 343.0 nm. Fluorescence/absorbance ratio = 26.

(+) 2′-O-MeCyd Adduct 2 (WF, Putative N-3 cis). UV λ_{max} [methanol]: 245.0, 279.0, 344.25 nm. Fluorescence/absorbance ratio = 7.

Preparation of dUMP Adducts. Adducts between dUMP and (+)-, (−)-, or (±)-*anti*-BPDE were prepared by the same procedure as dCMP adducts.

HPLC Analysis and Purification of Adduct Samples. Nonacetylated adducts were separated on a 25 cm × 0.4 cm Rainin Microsorb C_{18} column (Varian, Inc., Walnut Creek, CA) using a 42% methanol:water (0.8 mL/min) mobile phase. Adducts were detected by both absorbance (245 nm) and fluorescence (244 nm excitation and 400 nm emission). After one pass through the HPLC, the adducts were further purified by a second chromatography at 60% methanol:water using larger quantities per injection, to remove a contaminant (apparently derived from the HPLC column) that absorbs strongly at short wavelengths.

Peracetylated adducts were eluted from a 0.39 cm × 30 cm Waters Prep Nova-Pak HR Silica column with 1.0 mL/min 50% ethyl acetate:hexane (for the peracetylated NF cis adduct) or 80% ethyl acetate:hexane (for the peracetylated FL cis and trans adducts). Detection was by absorbance (345 nm) and fluorescence (344 nm excitation and 392 nm emission). Peak heights and areas were quantitated using Rainin Dynamax MacIntegrator hardware and software in conjunction with a Macintosh computer.

Measurement of Quantum Yields as a Function of Solvent Composition. To compare fluorescence quantum yields of samples analyzed at different times or with widely varying peak heights for this experiment, it was necessary to compensate for nonlinearity in fluorescence detector response and variations in detector response over time. Nonlinearity in detector response was appraised by generating a standard curve of detector response as a function of peak height from injections of varying amounts of *trans*-BPT. (Under the same conditions, the absorbance detector response was linear.) Variation in detector response over time was compensated for by measuring quantum yields in relation to that of a *trans*-BPT standard injected at the same time. The effect of mobile phase composition on tetrol quantum yield was measured by comparing a series of quantum yield measurements made in different mobile phases a few minutes apart.

Determination of pK_a Values. The pK_a values of the adducts were estimated by measuring aqueous−organic partitioning as a function of pH (*34*). Aliquots of a methanol solution of purified adduct were put into a series of vials, followed by removal of the solvent. The samples were dissolved in water-saturated 20% 1-butanol:ethyl acetate (0.5 mL). Then, 0.5 mL of aqueous buffer was added, and the sample was immediately vortexed for 90 s. The two phases were promptly separated with a Pasteur pipet, to ensure that the partitioning would not be influenced by any esterases produced by microbial activity. An additional 0.1 mL of butanol:ethyl acetate was then added to the organic phases to compensate for evaporation, and the adduct content of each phase was quantitated by UV absorbance. The buffers used ranged from pH 0.5 to pH 11.5. They were prepared with hydrochloric acid (pH 0.5), hydrochloric acid, and monobasic sodium phosphate (buffers from pH 1.0 to pH 2.5), citric acid and sodium succinate (pH 2.75−6.5), HEPES (pH 7.5), Tris HCl (pH 8.5), glycine (pH 9.5), and dibasic sodium phosphate (pH 10.5−11.5). In each case, solutions of the acid and either its sodium salt or the specified salt were mixed to give the desired pH. All solutions used except for hydrochloric acid were 50 mM.

Molecular Modeling. Several methods were used to calculate and minimize molecular potential energies. Molecular mechanics was performed using a modified version of N. L. Allinger's MM2 force field (*35*). Semiempirical molecular orbital calculations were performed using the PM3 Hamiltonian [Modified Neglect of Diatomic Overlap, Parametric Method Number 3 (*36*)] from MOPAC 97 (*37*) using the restrained Hartree−Fock method. Implicit solution-phase semiempirical molecular orbital calculations were performed with the aid of the COSMO method (*38*). All of these minimizations were performed using the software package Chem3D Pro 5.0 (CambridgeSoft Corp., Cambridge MA). Scripts for performing dihedral searches on an OS9 Apple Macintosh computer in conjunction with the molecular mechanics component of Chem3D may be obtained via the worldwide web (http://www.macinchem.fsnet.co.uk/).

Results

Relative Efficiencies of Alkylation of Poly(A), Poly(C), and Poly(G) by *anti*-BPDE. A rough idea of the relative efficiencies of the alkylation of different nucleic acid bases in polynucleotides by *anti*-BPDE was obtained from an experiment with ribonucleotide homopolymers and ^{3}H-labeled BPDE enantiomers. After extraction and dialysis, the proportions of added (+)-*anti*-

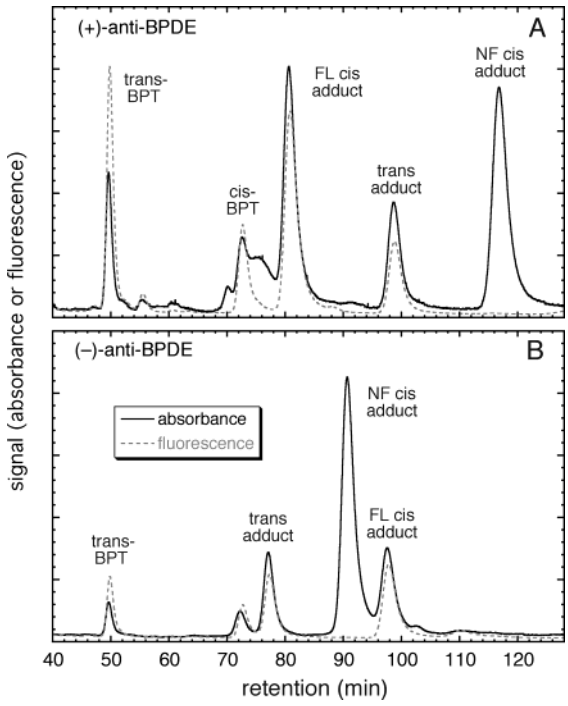

Figure 1. Reverse phase HPLC chromatograms of nonacetylated BPDE−dCyd adducts. (A) Adducts of (+)-*anti*-BPDE. (B) Adducts of (−)-*anti*-BPDE. Products were derived from the alkylation of dCMP by *anti*-BPDE at 23 °C in the absence of halide and subsequently converted to nucleosides. Adducts were eluted from a 25 cm C_{18} column with 0.8 mL/min of 42% methanol:water as described in the Experimental Procedures. Adduct elution was monitored by absorbance at 245 nm and by fluorescence using 244 nm excitation and 400 nm emission.

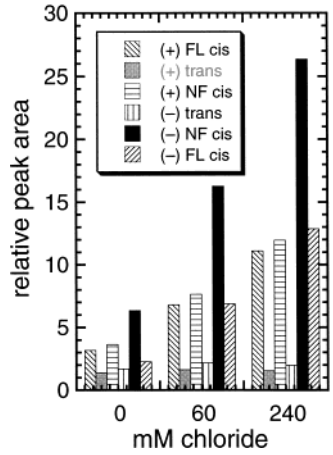

Figure 2. Effect of chloride ion on BPDE−dCMP adduct yield. Adducts were formed at the indicated chloride concentrations at 23 °C, isolated, and analyzed as described in the Experimental Procedures.

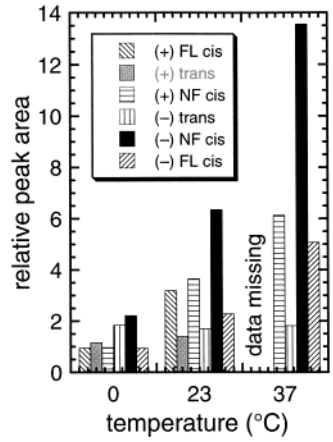

Figure 3. Effect of temperature on BPDE−dCMP adduct yield. Adducts were formed at the indicated temperature (in the absence of halide), isolated, and analyzed as described in the Experimental Procedures. The yields at 37 °C for the FL (+)-cis and (+)-trans adducts were not obtained.

BPDE remaining bound to 1 mg/mL samples of poly(A), poly(C), and poly(G) were 2.0, 0.55, and 18.2%, respectively. The corresponding figures for (−)-*anti*-BPDE were 2.3, 0.38, and 18.0%. Following alkali treatment and cartridge purification, the values were reduced to 1.4, 0.14, and 12.8% for (+)-*anti*-BPDE and to 1.7, 0.23, and 12.3% for (−)-*anti*-BPDE. The larger losses of poly(C) adducts may reflect a higher proportion of unstable and/or alkali labile adducts in these samples. Extrapolating these results to DNA would suggest that 1−2% of stable adducts are formed at dCyd, which is consistent with results obtained for denatured calf thymus DNA (*21*) and considerably lower than the proportions of dCyd adducts obtained from the (*S*,*R*,*R*,*S*) isomers of several other PAH epoxides (see Introduction).

Formation of dCyd Adducts. Each sample of nucleoside adducts obtained from reaction of dCMP with a single enantiomer of *anti*-BPDE contained three principal adduct peaks, as well as minor peaks and peaks due to residual tetrols. Sample chromatograms for adducts from (+)- and (−)-*anti*-BPDE are shown in Figure 1. Previous work in our lab has shown that the relative and absolute yields of cis *anti*-BPDE adducts are increased by the addition of halide to the reaction mixture (*9*−*13*) or by increasing the temperature of the reaction (*11*). The effects of chloride ion and temperature on adduct yield are shown in Figures 2 and 3, respectively. The effect of bromide on adduct yield is similar to that of chloride, except occurring over a 10-fold lower range of halide concentrations, and is shown in Figure S1 in the Supporting Information. For each BPDE enantiomer, two adduct peaks grow larger in both absolute and relative terms with increasing halide concentration or increasing temperature, while one adduct peak stays roughly the same size (and thus decreases from a relative standpoint). The peaks that increase with halide or temperature were identified as putative cis adducts, while those that do not were identified as putative trans adducts.

The efficiency of adduct formation with dCyd or dCMP was estimated by working up some dCyd adduct samples without extracting the tetrol hydrolysis products. Assuming that the extinction coefficients of adducts and tetrols are similar, adduct yields were calculated from the absorbance peak areas. For reaction of dCyd with (−)-*anti*-BPDE, the adduct yields are 4.0% at 0 °C, 6.5% at 23 °C, and 8.5% at 23 °C with 40 mM Cl^- present. For reaction of dCMP with (−)-*anti*-BPDE, the yields are 0.8% at 0 °C, 1.6% at 23 °C, 3.2% at 37 °C, and 4.0% at 23 °C with 60 mM Cl^-, 6.8% at 23 °C with 240 mM Cl^-, 3.2% at 23 °C with 4 mM Br^-, and 5.1% at 23 °C with 16 mM Br^-. The lower adduct yields obtained with dCMP as compared to dCyd may reflect a difference in prereaction physical complex formation or more effective catalysis of BPDE hydrolysis than alkylation by the phosphate group. Adduct formation with (+)-*anti*-BPDE followed similar trends but resulted in 25−55% higher yields than (−)-*anti*-BPDE with dCyd and lower yields (averaging 45% less) than (−)-*anti*-BPDE with dCMP (see

Table 1. Relative Fluorescence Yields of BPDE−dCyd Adducts[a]

	(+)-*anti*-BPDE		(−)-*anti*-BPDE	
adduct	F/A	SD	F/A	SD
trans	41.1	1.5	46.3	3.6
FL cis	47.2	3.4	41.4	3.5
NF cis	0.18	0.014	0.092	0.004

[a] Adducts were separated by reverse phase HPLC using 42% methanol:water and detected by fluorescence (244 nm excitation and 400 nm emission) and absorbance (245 nm) as described in the Experimental Procedures. The fluorescence to absorbance (F/A) peak area ratio of the adducts, normalized to a value of 100 for the highly fluorescent *trans*-BPT, is used as a measure of relative quantum yield. Values shown are means and standard deviations of three or more determinations.

Table S1 in the Supporting Information). These results suggest that the dCMP phosphate alters or interacts with the prereaction physical complex in a manner that discriminates against alkylation by the (+)-*anti*-BPDE enantiomer. This same discrimination may occur in DNA, as evidenced by preferential formation of dCyd adducts with (*S*,*R*,*R*,*S*) PAH epoxide enantiomers in all cases examined to date (*21*, *23*−*27*). Addition of I^- to reaction mixtures led to formation of destructive I_2, perhaps due to the presence of peroxides from THF. The longer and more rigorous dCMP workup would be expected to lead to a greater loss of the adducts initially formed, but this disadvantage was offset by the opportunity afforded to use organic extraction to remove tetrols and impurities from the BPDE sample that interfered with adduct HPLC.

We found in our experiment with ribonucleotide homopolymers that the alkylation of single-stranded poly(C) by each resolved enantiomer of *anti*-BPDE produces three adducts, just as for monomers. These adducts were detected by radioactivity, and because of the small sample sizes, their spectroscopic properties were not characterized. DNA adducts were not examined as part of this study.

Adduct Fluorescence Yields. In the adducts from both BPDE enantiomers, the trans adduct and one of the cis adducts have fluorescence quantum yields between 40 and 50% of that of *trans*-BPT, while the other cis adduct is virtually nonfluorescent (fluorescence yield 0.1−0.2% that of BPT; see Table 1). The ratio of the two types of cis adducts differs for (+)- and (−)-*anti*-BPDE. With (+)-*anti*-BPDE, the two cis adducts form in similar amounts. With (−)-*anti*-BPDE, the amount of NF cis adduct formed is more than twice the amount of FL cis adduct. For both *anti*-BPDE enantiomers, the trans adduct is generally least abundant (except in adducts formed in the absence of halide at 0 °C).

UV Spectra. The UV absorbance properties of the adducts also vary significantly. The UV spectra (Figure 4; Experimental Procedures) of each pair of corresponding adducts from the two BPDE enantiomers are virtually identical (Table S2 in the Supporting Information gives λ_{max} wavelengths for the adducts in methanol). The spectra of noncorresponding adducts differ significantly in terms of both λ_{max} and the shape of the spectrum. The long wavelength absorbance band is red-shifted 3 nm in the NF cis adducts and 1 nm in the FL cis adducts relative to the trans adducts (343.25 nm λ_{max}). Smaller shifts are seen in the 245 nm absorbance band. In this case, the NF cis adducts are red-shifted about 0.75 nm relative to the trans adducts (average λ_{max} = 245.9 nm),

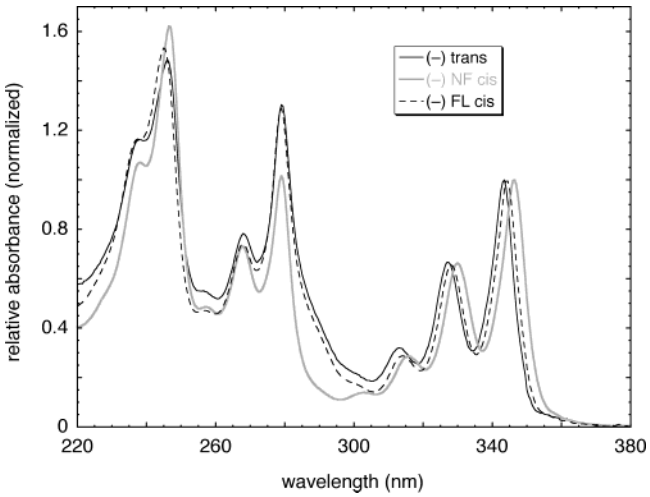

Figure 4. UV spectra of the dCyd adducts of (−)-*anti*-BPDE (in methanol). The absorbances are normalized to unity at the long wavelength maxima. The spectra of the adducts derived from (+)-*anti*-BPDE are virtually identical to those of the corresponding (−)-*anti*-BPDE adducts (see data in the Experimental Procedures).

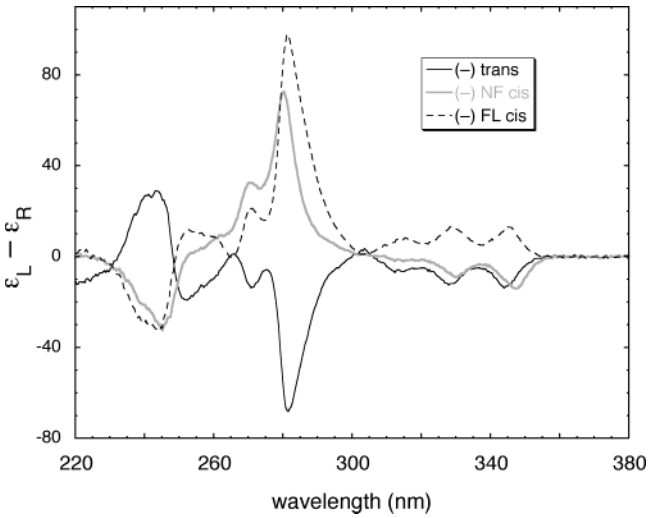

Figure 5. CD spectra of the dCyd adducts of (−)-*anti*-BPDE (in methanol). Calculation of $\epsilon_L - \epsilon_R$ is based on the assumption that the extinction coefficients of the adducts are the same as that of BPT (44 400).

while the FL cis adducts are blue-shifted an equal distance. The maxima of the 280 nm absorbance band are similar for all of the adducts (average = 279.0 nm). The relative intensities of different UV absorbance peaks are quite similar in the spectra of the trans and FL cis adducts, both of which differ significantly in this regard from the spectra of the NF cis adducts (Figure 4).

CD Spectra. In the CD spectra, the most prominent band for each dCyd adduct is near 280 nm. CD spectra of corresponding pairs of adducts from opposite BPDE enantiomers [spectra of adducts of (−)-*anti*-BPDE in Figure 5 and of adducts of (+)-*anti*-BPDE in Figure S2 in the Supporting Information] are, as expected, virtual mirror images of each other (*5*, *39*, *40*). The trans and FL cis adducts formed by a given BPDE enantiomer are approximate mirror images; they have ellipticities of opposite sign at all absorption bands, but the positions and shapes of the Cotton effects differ slightly. This is the expected relation for cis and trans adducts formed at the same alkylation site (*5*). The CD spectra of the

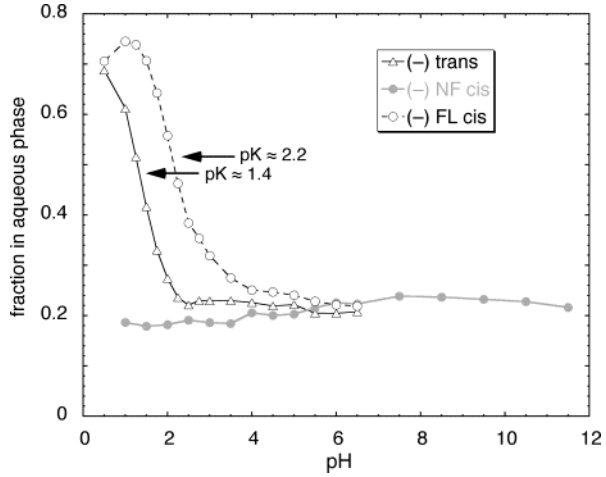

Figure 6. Aqueous−organic partitioning as a function of pH for the dCyd adducts of (−)-*anti*-BPDE. Adduct samples were allowed to equilibrate between equal volumes of 50 mM aqueous buffer and water-saturated 20% 1-butanol:ethyl acetate as described in the Experimental Procedures.

two cis adducts formed by a given BPDE enantiomer have ellipticities of the same signs at 245 and 280 nm but of opposite signs at 345 nm. Because the CD spectrum of a NF cis adduct is not an approximate mirror image of that of the trans adduct of the same BPDE enantiomer, one may conclude that it is formed by alkylation at a different site. Our CD spectrum of the trans dCyd adduct formed with (−)-*anti*-BPDE is consistent with the spectrum of a BPDE adduct obtained from denatured DNA and tentatively assigned the same structure (*16*).

pK_a Determination. The aqueous−organic partitioning of the dCyd adducts of (−)-*anti*-BPDE as a function of pH is shown in Figure 6. Deoxycytidine has a pK_a of 4.3 for protonation of the ring nitrogen (N-3) (*41*). The molecule acquires a positive charge below pH 4.3, which would cause a larger fraction to partition into the aqueous phase. The FL cis adduct has a pK_a of ∼2.2, about 2 pH units below that of dCyd. The pK_a of the trans adduct is ∼1.4, making its drop in pK_a relative to dCyd 40% greater than that of the FL cis adduct. The NF cis adduct shows no evidence of protonation down to pH 1.0. (The reduced aqueous fraction of the FL cis adduct at pH 0.5 probably results from the higher ionic strength of the solution used.)

Proton NMR Spectroscopy. Peracetylated adducts were prepared and purified by normal phase HPLC using an ethyl acetate:hexane mobile phase for use in obtaining NMR spectra. Retentions of these adducts varied remarkably. Under conditions in which nonacetylated *trans*-BPT has a retention of 31.5 min, the retentions of the peracetylated NF cis, FL cis, and trans dCyd adducts of (−)-*anti*-BPDE are 4.3, 19.6, and 22.3 min, respectively. Under these conditions, all three adducts also have a fluorescence yield greater than that of BPT (by factors of 1.7, 3.2, and 2.2, respectively).

NMR spectroscopy of peracetylated adducts was used to establish the alkylation sites of the trans and FL cis adducts. The NMR data for the (−)-*anti*-BPDE adducts are summarized in the Experimental Procedures and tabulated in the Supporting Information (see Tables S4−S6); the methine portion of the spectra of the (−)-cis adducts are shown in Figure 7, and the methine proton data for all of the (−) adducts is summarized in Table 2 (the aromatic portions of the spectra are displayed in Figures S4−S6 in the Supporting Information). In the cases of the (−)-trans and FL cis dCyd adducts, spectra taken before and after addition of D_2O to the sample revealed that a methine proton was coupled to an exchangeable proton, thus establishing the exocyclic amino group of dCyd (N^4) as the alkylation site and the former proton as H10 [the spectrum of the (−) FL cis adduct after deuterium exchange is given in Figure S3 in the Supporting Information]. In the case of the FL cis adduct, the coupling data were adequate to establish connectivity relationships. Less accurate coupling constants were obtained for the trans adduct due to smaller sample size. Two-dimensional homonuclear COSY was used to establish the methine proton connectivity of the trans adduct and confirm that of the FL cis adduct. The methine proton coupling constants also confirm the epoxide ring-opening geometries deduced from the CD spectra and the temperature and halide affects on adduct yield for these two adducts (see Discussion). The combination of coupling constants, COSY cross-peaks, and reference to the literature was adequate to allow identification of all proton resonances in the (−)-trans and FL cis dCyd adducts, except for the inability to distinguish between certain pairs of pyrenyl resonances.

In the case of the (−) NF cis adduct, an ^1H NMR deuterium exchange experiment showed that no methine proton is coupled to an exchangeable proton, establishing that alkylation is not at N^4. The most likely alternative in such a case is N-3, with O^2 being a secondary possibility. The ^1H NMR spectra of this adduct (in either acetone-d_6 or DMSO-d_6 for the peracetylated or nonacetylated forms, respectively) reveal two sets of resonances in an approximately 2:1 abundance ratio (the chemical shifts are tabulated in the Supporting Information; see Tables S5 and S6). Two-dimensional COSY and NOESY spectra were obtained in both solvents.

The NOESY spectra of the NF cis adduct (see Figure S7 in the Supporting Information) indicate that the two sets of resonances are related through chemical exchange, thus establishing that this adduct exists in two conformations. The minimum separation observed for corresponding peaks indicates that the exchange rate for the peracetylated adduct in acetone-d_6 at 25 °C is slower than 25 Hz (similar results were obtained for the nonacetylated adduct in DMSO-d_6 at 30 °C). At 80 °C, observations of peak coalescence in spectra of the nonacetylated adduct in DMSO-d_6 indicate an exchange rate of roughly 500 Hz. Combining this with a rate of 25 Hz at 25 °C yields an estimate of 11.4 kcal/mol for the energy barrier, so the actual value must be somewhat higher.

The presence of two conformers is most reasonably interpreted as pointing toward alkylation at N-3. Alkylation at this site puts the pyrimidine and hydrocarbon benzo rings one bond apart, thereby creating steric constraints that could inhibit rotation of the pyrimidine ring (see below). Alkylation at O^2 would leave the rings separated by two bonds, just as for alkylation at N^4. The COSY and NOESY spectra permit assignment of the peaks for each proton of both conformers in acetone-d_6.

Effect of Methyl Protection on Cyd Adduct Formation. To obtain additional evidence for the location of the alkylation site in the NF cis adducts, (+)-*anti*-BPDE was reacted with cytidine, 2′-O-methylcytidine, and 3-methylcytidine. The cytidine reaction gave two

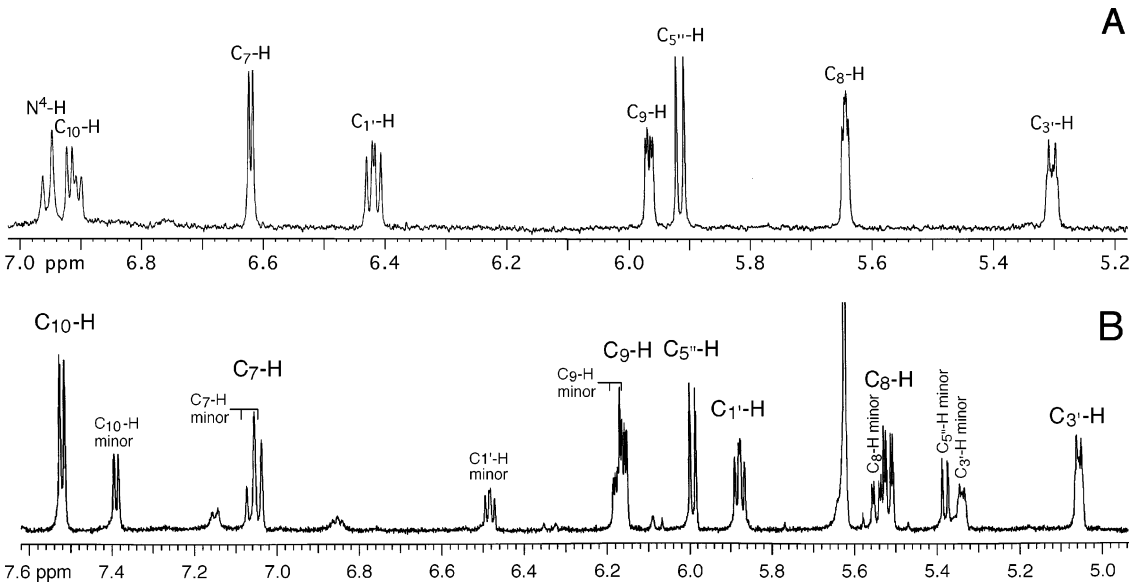

Figure 7. Methine proton region of the 600 MHz ^{1}H NMR spectra (in acetone-d_6) of the per-O-acetylated FL cis dCyd (A) adduct or NF cis dUrd adduct (B) formed by (−)-*anti*-BPDE.

Table 2. NMR Spectral Data for Methine Protons of Per-O-Acetylated BPDE−dCyd Adducts (in Acetone-d_6)

	chemical shift (ppm)				
adduct	H7	H8	H9	H10	N^4−H
(−)-trans	6.78	5.73	5.98	6.44	7.63
(−) FL cis	6.62	5.64	5.97	6.91	6.95
(−) NF cis[a]	7.05	5.52	6.16	7.52	
(−) NF cis[b]	7.06	5.55	6.18	7.39	
	coupling constants (Hz)				
	J(7,8)	*J*(8,9)	*J*(9,10)	*J*(10,N)	
(−)-trans	∼9.7	∼1.7	∼2.6	∼7.9	
(−) FL cis	4.1	2.29	4.94	9.06	
(−) NF cis[a]	10.25	3.29	6.96		
(−) NF cis[b]	∼10.7	∼3.1	6.22		

[a] Major conformer. [b] Minor conformer.

adduct peaks with fluorescence yields and UV absorption spectra similar to those of the trans and NF cis adducts of dCyd (Figure 8A and Experimental Procedures; see Table S3 in the Supporting Information for absorption λ_{max} and fluorescence yield data). The reverse phase HPLC retentions are shorter than for the corresponding dCyd adducts, as would be expected. An adduct corresponding to the FL cis product was not visible, due to elution close to *trans*-BPT, the major BPDE hydrolysis product. (The large tetrol peaks in the samples obtained with nucleoside starting material resulted from omission of an organic extraction step in order to avoid losses of the uncharged adducts. However, the putative N^4 cis adduct peak was observed in an adduct sample obtained from CMP.)

The 3-methylcytidine reaction yielded a peak corresponding to the trans adduct but not one corresponding to the NF cis adduct (Figure 8B). (A very small peak with a low fluorescence yield is visible in the chromatogram, possibly due to the presence of a small amount of nonmethylated cytidine in the sample.) The 2′-O-methylcytidine reaction yielded a peak with properties similar to those of the other putative cytidine trans adducts and a second (WF) peak with a reduced fluorescence yield intermediate between those of the trans cytidine adducts and the NF cytidine adduct (Figure 8C and Table S3 in the Supporting Information). The latter peak was broader than the others and seemed to exhibit a more variable retention time. We surmise that this represents the N-3 adduct, whose conformation and/or dynamics are altered by the presence of the 2′-O-methyl group so as to reduce the quenching of the hydrocarbon by the base. The UV red shift of this adduct is less than that of the NF cis adducts (λ_{max} at 344.25 nm vs 346.25 nm for the NF cis BPDE−cytidine adduct, as compared to 342.0−342.5 nm for the three trans cytidine and methylcytidine adducts; see the Experimental Procedures and the Supporting Information), which suggests that base−hydrocarbon stacking interactions are reduced. The fact that only the 3-methylcytidine reaction failed to yield an adduct with reduced fluorescence again points to N-3 as the alkylation site in the NF cis adduct.

Comparison of dUrd and dCyd Adducts. Because N-3 adducts of dCyd have been reported to deaminate in a number of cases (*42*−*52*), adducts were generated between dUrd and both enantiomers of *anti*-BPDE. These samples contained adducts with the same retentions and spectroscopic characteristics as the NF cis adducts of dCyd. Figure 9 depicts a coinjection experiment demonstrating the identity of the NF adduct formed by (−)-*anti*-BPDE and dCyd and the principal product formed by (−)-*anti*-BPDE and dUrd.

Mass Spectrometry. High-resolution EI-MS of the peracetylated NF cis adduct confirmed that deamination had occurred. These spectra did not yield a molecular ion but rather yielded the molecular ion minus one or two acetyl groups. The molecular ion of the nonacetylated form of this adduct was obtained by electrospray. Results obtained by mass spectrometry for the trans and FL cis dCyd adducts were also consistent with expectations (see Experimental Procedures).

Adduct Structures. The structures proposed for the three adducts formed between (−)-*anti*-BPDE and dCyd are shown in Scheme 1. The epoxide ring-opening geometries shown were determined most definitively by the sign of the major CD band. The N^4 alkylation sites of the trans and FL cis dCyd adducts were established by NMR deuterium exchange experiments, while alkylation experiments using methyl-protected cytidine derivatives as

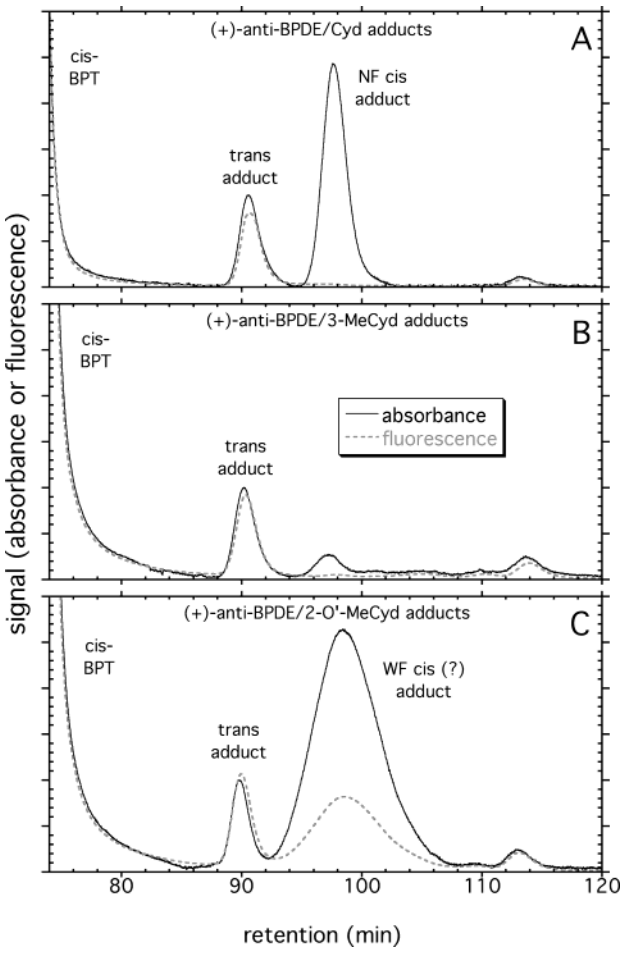

Figure 8. Reverse phase HPLC chromatograms of adducts derived from the alkylation of cytidine or methylated cytidine derivatives by (+)-*anti*-BPDE. (A) Adducts derived from cytidine. (B) Adducts derived from 3-methylcytidine. (C) Adducts derived from 2′-O-methylcytidine. Products were formed at room temperature in 30 mM KBr. Adducts were eluted from a 25 cm C_{18} column with 0.8 mL/min of 42% methanol:water as described in the Experimental Procedures. Retentions have been normalized to adjust for small variations in solvent composition and pump output. Adduct elution was monitored by absorbance at 245 nm and by fluorescence with 245 nm excitation and measuring emission above 320 nm with a cutoff filter. Signal ranges have been normalized to give uniform heights to the absorbance signal of the trans adducts. Under the same conditions, the retentions of *trans*-BPT and the FL cis adduct of (+)-*anti*-BPDE with Cyd are 49.6 and 52.3 min, respectively.

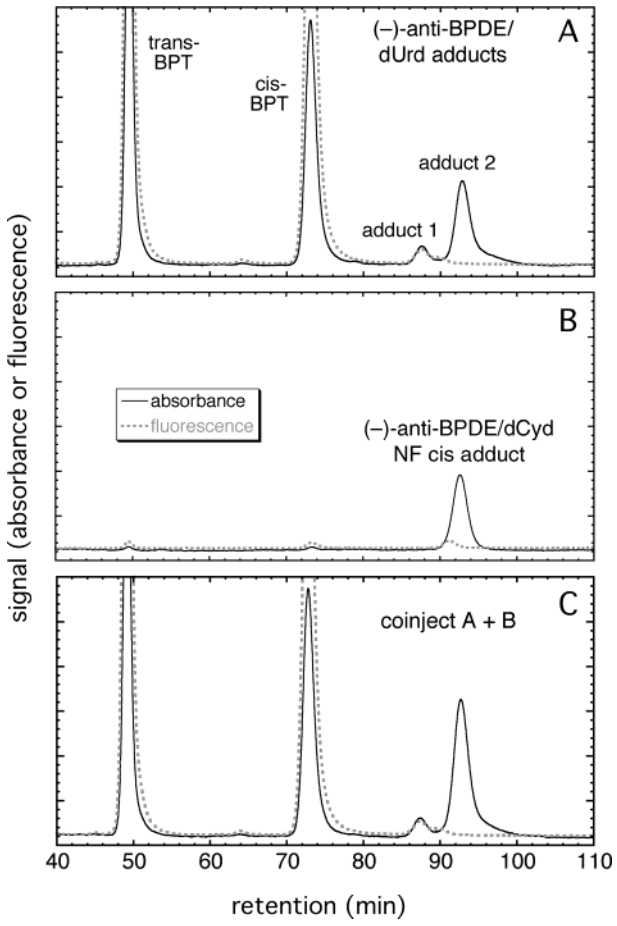

Figure 9. Comparison of reverse phase HPLC chromatograms of the dUrd adducts and NF cis dCyd adduct of (−)-*anti*-BPDE. (A) Deoxyuridine adducts. (B) Purified NF cis dCyd adduct. (C) Coinjection of A + B. dUMP adducts were formed at 0 °C in the absence of halide and subsequently converted to nucleosides. Adducts were eluted from a 25 cm C_{18} column with 0.8 mL/min of 42% methanol:water as described in the Experimental Procedures. Retentions have been normalized to adjust for small variations in solvent composition and/or pump output. Adduct elution was monitored by absorbance at 245 nm and by fluorescence using 246 nm excitation and 392 nm emission. Under the same conditions, the retentions of the NF cis and putative trans adducts of (+)-*anti*-BPDE and dUrd are 119 and 97 min, respectively.

well as the NMR evidence for two conformers point to N-3 as the NF cis dCyd adduct alkylation site. The dUrd adduct cochromatography, mass spectrometry results, and the pK_a determination (see Discussion) all indicate that the latter adduct deaminates to the corresponding dUrd adduct. This further supports alkylation at N-3, because no deamination would be expected for an O^2 adduct.

Solvent Effect on Adduct Fluorescence. To obtain more information on the fluorescence properties of the NF cis adduct, the quantum yields of the two cis adducts of (−)-*anti*-BPDE, as well as of *trans*-BPT, were measured in air-saturated methanol−water mixtures varying from 40 to 80% methanol (see Figure 10). The measurements were made on peaks eluting from an HPLC column, to avoid artifacts associated with BPT or other high quantum yield decomposition products of the adducts. The quantum yield of BPT decreased monotonically with increasing methanol content. The fluorescence yield of the FL cis dCyd adduct increased over the range of 40−60% methanol and then decreased, while that of the NF cis dCyd adduct increased monotonically. Oxygen quenching is expected to cause a decrease in yield principally above 50% methanol (*53*). Relative to the tetrol, the yields of both cis adducts increased roughly linearly with increasing methanol content, with the FL adduct increasing 2.5-fold over the range tested and the NF adduct increasing 12-fold. The increase in the relative emission of the adducts with increasing methanol is consistent with an intramolecular electron transfer-based quenching mechanism (see Discussion) (*53*).

Conformations of the N-3 dUrd Adduct. The methine proton NMR coupling constants indicate that in both conformers of the cis N-3 dUrd adduct of (−)-*anti*-BPDE the C-7 and C-8 substituents are quasi equatorial and the C-9 substituent is quasi axial. The NOESY spectrum indicates that H_8 and H_{10} are roughly diaxial in both conformers. This conformation is quite different

Scheme 1. Proposed Structures of Adducts Formed between (−)-*anti*-BPDE and Deoxycytidine[a]

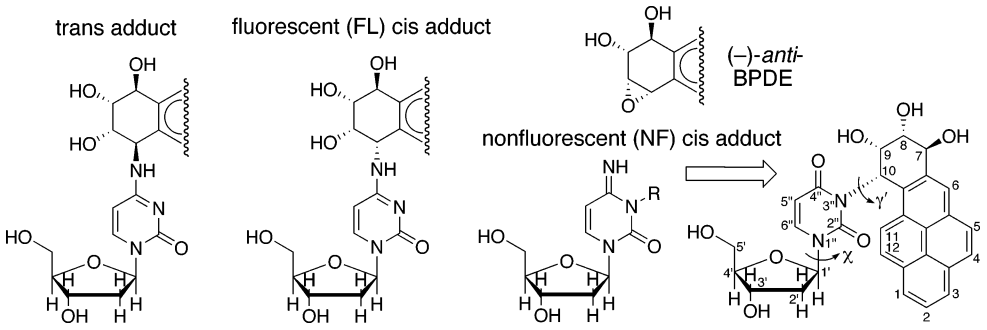

[a] Torsion angles χ and γ' are defined as C2″-N1″-C1′-O4′ and C9-C10-N3″-C2″.

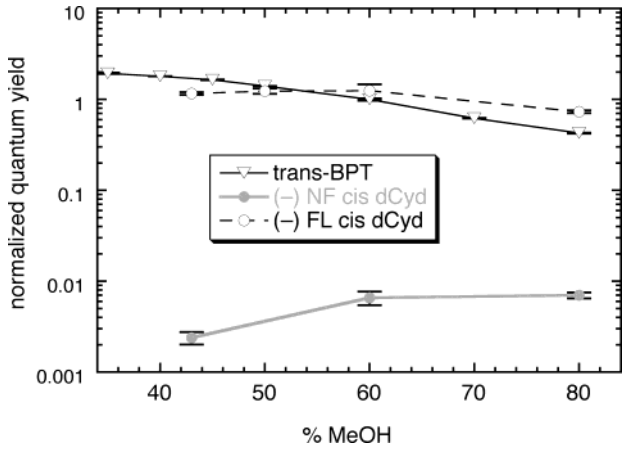

Figure 10. Fluorescence quantum yields as a function of methanol concentration for *trans*-BPT and the FL and NF cis dCyd adducts of (−)-*anti*-BPDE. Adducts were eluted from a 25 cm C_{18} column with 0.8 mL/min using air-saturated methanol:water mixtures of varying proportions. Quantum yields were measured using peak heights for fluorescence (246 nm excitation and 392 nm emission) and absorbance (245 nm) as described in the Experimental Procedures. All quantum yields have been normalized to a value of unity for *trans*-BPT at 60% methanol: water. Values represent mean ± standard deviation for three or more determinations.

from that of the cis N^4 adduct (see Discussion). As compared to the NMR spectrum of the minor conformer, the spectrum of the major conformer shows 0.3−0.8 ppm upfield shifts at the sugar resonances and a 0.6−0.7 ppm downfield shift for H5″ of the pyrimidine (see Figure S8 in the Supporting Information). This could be explained if the sugar moiety of the major conformer and $H_{5''}$ of the minor conformer were shielded by being situated above the pyrenyl ring system (with contributions from deshielding of the minor conformer sugar and major conformer $H_{5''}$).

Molecular Modeling of the Uracil Adduct. Candidate structures for the two observed conformers of the N-3 adduct of (−)-*anti*-BPDE were identified through a gas phase conformational search employing molecular mechanics (see Experimental Procedures). Initially, the problem was simplified by considering only the nonacetylated N-3 uracil adduct. Multiple conformers have not been observed for exocyclic amino group adducts of *anti*-BPDE, so it is reasonable to assume that the conformers of the N-3 dCyd adduct result from barriers to rotation of the pyrimidine ring with respect to the attached hydrocarbon.

The conformational space of the uracil adduct was examined by rotating the pyrimidine ring using one of the four dihedral angles associated with the bond between C-10 of the hydrocarbon and N-3 of the pyrimidine. The results (see Figure S9 in the Supporting Information) are presented in terms of the γ' dihedral (defined in Scheme 1) and the δ' dihedral, defined as pyrenyl-C10-N3″-C4″ (chosen to minimize the effects of benzo ring distortion). Molecular potential energy varies with both the choice of dihedral and the direction of rotation. The locations and energies of the minima are reasonably consistent, while those of the maxima vary widely. A more detailed description of the procedure, plots of the results, conformations of minima, and movies of sample dihedral rotations are included in the Supporting Information.

Two minimal energy conformations consistent with the NMR evidence for benzo ring proton orientations were identified and minimized further after release of the dihedral constraints. They are located at γ' values of −94 and 82° and have energies of −18.2 and −18.7 kcal/mol, respectively. The two conformations are similar but differ by a 180° rotation of the pyrimidine. The C-7, C-8, C-9, and C-10 hydrogens are (quasi) axial, axial, equatorial, and intermediate, respectively (the C-8 and C-10 hydrogens are close to parallel). The minima are characterized by a 69° angle between the planes of the pyrimidine and pyrenyl moieties, benzo ring conformations with C-8 and C-9 displaced out of the plane away from and toward the pyrimidine, respectively, and by a favorable dipole/dipole and dispersive interaction between the C-9 hydroxy and one of the uracil carbonyls. Two additional minima with benzo ring conformations inconsistent with the NMR results were also found and are described in the Supporting Information.

The calculated rotational energy barriers between successive uracil adduct minima average 31 kcal/mol in height and range from 11.5 to 58 kcal/mol, consistent with the exchange rates inferred from NMR. The peaks generally correspond to the points of maximum strain induced by proximity of a pyrimidine carbonyl to the C-9 hydroxy (or occasionally the C-8 hydroxy). The highest barriers represent situations where the dihedral driver traps the pyrimidine ring below the pyrenyl moiety and are not relevant to the molecular dynamics. The actual barrier height is probably closer to the low end of the range.

Molecular Modeling of the Deoxyuridine Adduct. The Ura adduct minima were used to search for nonacetylated dUrd adduct minima by appending a C2-endo deoxyribose to both structures and using a dihedral search to rotate the sugar while constraining the pyrenyl−pyrimidine dihedral. For both pyrimidine orienta-

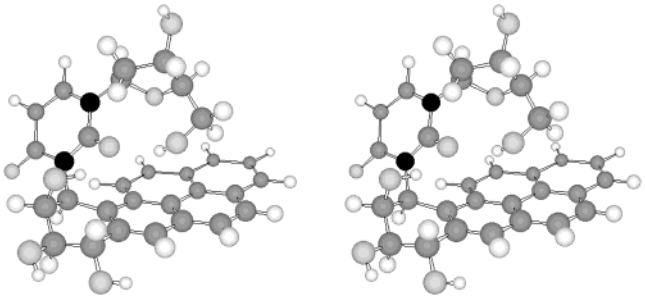

Figure 11. Stereoview of the gas phase minimum energy conformation of the major conformer of the N-3 dUrd adduct derived from alkylation of dCyd by (−)-*anti*-BPDE as obtained from molecular mechanics. Conformations of additional minima are available in the Supporting Information.

tions, a single well-defined minimum was observed at a χ value in the 50−60° range, i.e., at a syn orientation of the glycosidic bond (see Figure S10 in the Supporting Information). This minimum occurs when the sugar orientation permits interactions between the C5′-OH and the C2″ carbonyl of the uracil (the molecular mechanics force field used may exaggerate the strength of such interactions). Energy barriers for rotating the sugar away from the minimum range from 8.5 to 16 kcal/mol. The dUrd adduct minima were refined by further minimization with all constraints removed. This yielded the final conformations with γ' angles of −94 and 88°, χ angles of 52 and 56°, and steric energies of −7.1 and −13.4 kcal/mol for the putative minor and major conformers, respectively (coordinate information and images of the minima conformations are given in the Supporting Information). The pyrimidine−hydrocarbon plane angle is 69° in the former case (the same as for the corresponding Ura adduct) and a more acute 54° in the latter case (see Figure 11). In the major conformer, interactions between the C5′-OH and the hydrocarbon lower the steric energy and pull the sugar and pyrimidine closer to the hydrocarbon. Sugar−hydrocarbon interactions are not possible in the minor conformer.

The 6.3 kcal/mol energy difference between the two dUrd adduct minima calculated with molecular mechanics is considerably larger than the 0.4 kcal/mol difference implied by the observed 1:2 conformer abundance ratio. The force field used evidently exaggerates the strength of the dispersive sugar−hydrocarbon interactions. Further minimization with semiempirical quantum mechanics yields an energy difference of 1.2 kcal/mol in a vacuum, and differences smaller than 0.4 kcal/mol in implicit solvent with the dielectric constant of acetone-d_6, DMSO-d_6, or water. These minimizations turn the pyrimidine ring clockwise (when viewed from above) and swing it up to a more orthogonal position with respect to the pyrenyl moiety (similar changes were seen in semiempirical quantum mechanical minimizations of the Ura adduct). Details are provided in the Supporting Information.

Discussion

The task of structure determination for a given BPDE adduct consists of identifying the BPDE enantiomer involved, the epoxide ring-opening geometry, the target alkylation site, and any postalkylation chemical changes that may have occurred. We established the stereochemistry of ring opening for the BPDE−dCyd adducts by a combination of four types of measurements: the halide effect on adduct yield, the temperature effect on adduct yield, the sign of the major CD band, and the NMR coupling constants of the methine protons of the BPDE benzo ring. Examination of halide and temperature effects on adduct formation facilitated the stereochemical assignments in this case and should be useful in the analysis of other PAH epoxide products. Although these methods might not be considered definitive, they are rapid (since adduct purification is not necessary) and require very little material. In the case of the N-3 adduct, the halide and temperature effects proved to be more reliable guides to ring-opening geometry than an accepted rule based on benzo ring NMR coupling constants.

Previous work in our lab has shown that the formation of cis *anti*-BPDE products is catalyzed by halide ions (*9*−*13*). The halide effect arises from partial conversion of BPDE into a trans halohydrin. The trans halohydrin can be formed by halide attack on C-10 of either BPDE or its carbocation. The trans halohydrin then alkylates the same targets as BPDE, by a mechanism involving inversion of configuration at C-10, leading to cis adduct formation. This reaction pathway competes with the S_N1 pathway by which BPDE alkylates targets in the absence of halide catalysis. We have synthesized the putative chlorohydrin intermediate of the chloride-catalyzed pathway (*13*) and shown that in the case of dAdo alkylation it generates twice the proportion of cis products as BPDE in the absence of salt (65 vs 35%) but the same proportion of cis adducts as BPDE at high levels of chloride (88%) (*12*). The relative catalytic potency of halides follows the order $I^- > Br^- > Cl^- \gg F^-$.

The proportion of cis products produced by BPDE can also be increased by raising the reaction temperature (*11*). This effect is reduced in the presence of halides. Evidently, in the nonhalide-catalyzed S_N1 pathway of product formation, the activation energy for the formation of cis products is higher than that for trans products. The effect can be explained in terms of an equilibrium believed to exist between alternative conformations of the benzo ring of BPDE (*5*, *54*, *55*). A higher energy, more reactive conformer with quasi axial C-7 and C-8 hydroxy groups may form cis products, while a lower energy quasi equatorial conformer may be the precursor to trans products. The relative abundance of the cis precursor conformer would increase with temperature. There are analogous pairs of conformers of the trans chlorohydrin derivative of BPDE, as well as of the C-10 carbocation formed by both BPDE and its chlorohydrin. It has recently been proposed that halide ions increase the proportion of cis products by catalyzing the interconversion of the two carbocation conformers, which are not in equilibrium in aqueous solution in the absence of external halide due to their short lifetimes (*56*). The ratio of conformers produced by the chlorohydrin in the absence of halides is believed to be closer to the equilibrium ratio (which favors cis product formation the most) than the ratio produced by BPDE.

A general correlation has been noted between the CD spectra of purine nucleoside adducts of PAH diol epoxides and the absolute configuration at the benzylic carbon of the hydrocarbon attached to the purine (*2*). A positive major CD band is associated with *S* stereochemistry and a negative major CD band with *R* stereochemistry. Thus, for BPDE adducts, the major CD band should be positive for (−)-cis or (+)-trans adducts and negative for (+)-cis

or (−)-trans adducts. This rule may be ambiguous if there is no clearly dominant band, but the BPDE−dCyd adducts have an obviously dominant CD band at 280 nm. Because our dCyd adducts were made with pure enantiomers of *anti*-BPDE, the assignment of absolute configuration at C-10 by CD specifies the ring-opening geometry (assuming the rule is equally applicable to pyrimidine nucleoside adducts).

Determination of the epoxide ring-opening geometries of the adducts by ^{1}H NMR coupling constants (*5*, *22*) is believed possible because of differing half-chair benzo ring conformations in cis and trans adducts, which are apparently retained from their precursor BPDE conformers. In cis adducts, the orientation of the C-7, C-8, and C-10 substituents is normally quasi axial, resulting in coupling constants of about 3.2−4, 2.1−2.5, and 5−5.7 for *J*(7,8), *J*(8,9), and *J*(9,10), respectively. In trans adducts, the C-9 and C-10 substituents are generally quasi axial, and the C-7 and C-8 substituents are quasi equatorial, and the corresponding coupling constants have values of 9, 1.9−2.5, and 2.5−4. The *J*(7,8) and *J*(9,10) coupling constants have thus been considered diagnostic for cis and trans *anti*-BPDE adducts. Our NMR results indicate that this rule is valid for N^4 dCyd adducts but not N-3 dUrd adducts. In an N-3 dUrd adduct, the uracil moiety is unable to assume a fully axial conformation because of steric clashes between its carbonyl groups and the hydrocarbon. The interaction between the C-9 hydroxy and the uracil carbonyls may also influence cis dUrd adduct benzo ring stereochemistry.

A correlation that can be drawn between the methine proton chemical shifts and the epoxide ring-opening geometry in every *anti*-BPDE adduct ^{1}H NMR spectrum previously reported is that the H7 resonance is farther downfield than the H10 resonance in trans adducts, while the opposite occurs in cis adducts. This relationship holds true in the adducts tested here.

In summary, the epoxide ring-opening geometries of the adducts were assigned by the halide effect in six cases, by the temperature effect in six cases, and by the sign of the major CD band in six cases. All of the assignments by these three methods are consistent. For products of (−)-*anti*-BPDE, the NMR coupling constant rule gives the correct stereochemistry for the two N^4 adducts but fails in the case of the N-3 adduct.

The alkylation sites of the dCyd adducts of (−)-*anti*-BPDE were established by deuterium exchange NMR experiments in two cases and in the third case by inferences drawn from spectroscopic properties, alkylation experiments with selectively protected nucleosides, the occurrence of deamination, and the presence of two conformers. The deuterium exchange experiments establish N^4 as the alkylation site for the trans and FL cis adducts, because this is the only exchangeable base site. For these exocyclic amino group dCyd adducts, the relative reverse phase retentions of the trans and cis adducts of a given BPDE enantiomer are the same as for dGuo adducts [trans first for (−)-BPDE, cis first for (+)-BPDE] and opposite that of dAdo adducts.

Because we observed formation of all four expected N^4 dCyd adducts (cis and trans for each BPDE enantiomer), the additional (NF) cis adduct for each BPDE enantiomer must be alkylated at another site. This conclusion is supported by the CD spectra of the adducts. The most obvious alternative is the ring N-3 position, the site most often attacked when cytidine is reacted with simple alkylating agents in neutral solution (*57*); O^2 adducts can also be formed (*58*).

Early work on cytidine alkylation showed that N^4/N-3 selectivity is influenced by the type of nucleophilic addition. Methyl iodide was found to give almost exclusively the N-3 product in neutral DMSO, while the ethyl iodide reaction yields a 21:1 N-3: N^4 product ratio (*59*). When the ethylating agents $EtMeSO_3$ or Et_2SO_4 are reacted with cytidine or poly(C) in neutral aqueous solution (*57*), 12−18% of the ethylation is at N^4, with most of the balance at N-3. The carcinogenic alkylating agent 7-bromomethylbenz[*a*]anthracene gives an N-3 adduct when reacted with cytidine in dimethylacetamide (*60*) but gives a 9:7 ratio of N-3 to N^4 cytidine adducts in neutral aqueous solution (*61*). In aqueous buffer, benzyl bromide gives 87% N-3 cytidine adducts, while paramethoxybenzyl bromide gives exclusively N^4 adducts (*61*). It appears that N^4 as opposed to N-3 alkylation is favored by circumstances that stabilize a positive charge on the alkylating agent and shift the product distribution from kinetic to thermodynamic control (*61*), i.e., by a reaction with greater S_N1 as opposed to S_N2 character. A similar observation has been made regarding N^2 vs N-7 alkylation of dGuo (*62*).

In more recent work, deamination of N-3 dCyd adducts has been observed in a number of cases both with free nucleoside and in DNA (*42*−*52*). In each of these instances, as in the case reported here, the second carbon from N-3 in the alkylating moiety bears a hydroxy group, which appears to catalyze the process. The deamination of 3-hydroxyethyl-Cyd is 60-fold more rapid than that of 3-ethyl-Cyd (*45*). The hydrolysis of the intermediate imine is also catalyzed by alkali (*45*). Half-lives reported for hydroxyalkyl N-3 dCyd adducts at pH 7.4 and 37 °C have ranged from 6 min to several hours (*49*, *51*). Two mechanisms have been proposed for the deamination (*42*, *48*, *51*); in the favored mechanism, the adduct hydroxy group attacks cytosine C-4 of the imine, releasing ammonia and generating a five member oxazolinium ring intermediate that is then hydrolyzed.

There is no precedent for adduct formation at O^2 of dCyd by a PAH epoxide. O-alkylation is favored by S_N1 alkylation reactions involving "hard" electrophiles with a localized positive charge, whereas exocyclic amino group alkylation is favored for "soft" electrophiles with a delocalized charge, such as PAH dihydrodiol epoxides (*62*). O^2 adducts of dCyd are unstable and subject to depyrimidation (cleavage of the glycosyl bond) by a pH-independent mechanism (*63*); O^2 adducts of Cyd are significantly more stable. Alkylation of dCyd at O^2 by methyl and ethyl *N*-nitrosoureas (*58*, *63*, *64*) yields adducts with a half-life of 26 h in aqueous solution at neutral pH (*63*); the corresponding butadiene monoxide adducts have a half-life of 11 h (*49*).

It was expected that the pK_a value of an adduct would shift relative to that of dCyd (pH 4.3) in a manner dependent in part on the alkylation site. When the site of protonation is not directly modified, pK_a could be affected through inductive effects, effects on pyrimidine resonance/tautomeric equilibria, or by steric inhibition of hydration at the protonation site. In the N^4 adducts, the site of protonation would be N-3, as for unmodified dCyd. Alkylation at N-3 generates an imine at N^4 that would be positively charged at neutral pH [the pK_a of 3-ethyl-dCyd is 8.6 (*59*)]. Alkylation at O^2 also raises the pK_a of dCyd [the pK_a of O^2-ethyl-dCyd is over 9.5; this

would drop to 5.4 following depyrimidation (*63*)]. Like its parent nucleoside, a dUrd adduct would not be expected to exchange protons over the pH range 0−13 (*41*).

Both the aromatic and the hydroxy substituents of the hydrocarbon moiety are electron withdrawing and would tend to lower the pK_a. Inductive effects fall off rapidly with distance and are seldom observable over a range of more than four bonds. Such effects on N-3 protonation in N^4 dCyd adducts should be modest, as they would have to be transmitted over three intervening atomic centers from the pyrenyl moiety or four from the C-9 hydroxy group.

The observed drops in the pK_a values of the trans and FL cis adducts relative to dCyd (2.9 and 2.1 units below 4.3, respectively) are more than would be expected from induction. A similarly low pK_a (1.7 units below dCyd) has been reported for the trans N^4 dCyd adduct of dibenz-[*a*,*j*]anthracene 3,4-diol 1,2-epoxide (*18*). The pK_a of N^4-ethylated deoxycytidine is unchanged at 4.2 (*25*). Because the inductive effect would be the same for both N^4 BPDE−dCyd adducts, the difference must be wholly due to an additional effect. Steric inhibition of cation solvation by the hydrocarbon moiety, which could vary with adduct conformation, may be responsible. This effect would stabilize the uncharged form, which in the case of dCyd adducts is the unprotonated form, thus lowering their pK_a values. The pK_a of the trans BPDE−N^2−dGuo adduct (*65*) is consistent with this viewpoint. The pK_a for N-1 protonation on this adduct is 9.8 vs 9.16 for unmodified guanosine. This increase is opposite what would be expected from induction. However, stabilization of the uncharged form, which in this case is the protonated form, could account for the shift.

By limiting the freedom of the base and hydrocarbon to move with respect to each other, N-3 alkylation should favor base−hydrocarbon interactions from an entropic standpoint. The strong quenching of the hydrocarbon fluorescence in the NF cis adducts and the red shift of their UV absorption spectra imply that the base−hydrocarbon interactions are stronger in N-3 than in N^4 adducts. Somewhat larger red shifts (up to 10 nm) are observed when pyrenyl moieties are intercalated in DNA, with (*66*) or without (*67*, *68*) covalent attachment, and also as a consequence of noncovalent stacking interactions between a hydrocarbon and one (*69*) or two[3] nucleosides.

The mechanism of quenching in the BPDE−dCyd adducts is probably similar to that observed in stacked dCyd−BPT physical complexes (*70*). In these complexes, quenching results from electron transfer from the hydrocarbon to the pyrimidine, resulting in the formation of a BPT radical cation. The electron transfer is facilitated by a rapid coupled proton transfer from water to the pyrimidine radical anion. The proton transfer requirement explains why dCyd adduct quenching would not be observed in ethyl acetate:hexane solvent mixtures. In water−methanol mixtures, solvent stabilization of the hydrocarbon radical cation would decrease with increasing methanol concentration, which would tend to increase emission (*53*). A decrease in hydrophobic base−hydrocarbon stacking interactions with increasing methanol would have a similar effect. In BPT−dGuo physical complexes or in BPDE−dGuo adducts, quenching results from electron transfer in the opposite direction, from the purine to the hydrocarbon, due to the differing redox potentials of the two nucleosides.

The molecular mechanical investigation that we performed on the conformation space of the cis N-3 dUrd adduct explained the presence of two conformers of this molecule in terms of the existence of two minima of very similar energies, corresponding to pyrimidine orientations differing by a half-turn, separated by significant energy barriers. Similar but much more extensive searches of conformation space have been performed for the exocyclic amino adducts of dGuo (*71*, *72*) and dAdo (*73*, *74*) with *anti*-BPDE by the Broyde group. There are significant differences between the influences and the constraints governing the conformations of the N-3 dUrd adduct and those influencing the purine adducts. The structure of the base aromatic ring adjacent to the point of linkage to the hydrocarbon is symmetric for an N-3 uridine adduct but not for the purine adducts. In the former case, the aromatic ring of the base is separated by one rather than two bonds from the hydrocarbon's benzo ring, so rotation of the base would lead to greater distortions of benzo ring conformation in the dUrd adduct. Interactions between base carbonyls and hydroxy groups of the benzo ring or sugar are possible in the dUrd adduct but not in the purine adducts where the base either has no carbonyl group (dAdo) or has one that is too distant (dGuo). Additionally, sugar−hydrocarbon interactions are less likely in the purine adducts, due to the greater distance between the moieties, although they do occur [e.g., domain IV for the trans dGuo adduct (*71*), domain V for the cis dAdo adduct (*74*)]. In the lowest energy dGuo adducts, the glycosidic bond is in an anti orientation, while it is syn in the most favored dAdo adducts. It is also syn in our minima conformations for the *cis* N-3 dUrd adduct. The γ' angle in the *cis* N-3 dUrd adduct is the dihedral most nearly analogous to the β' angle defined by Broyde et al. for the BPDE−purine adducts (in both cases, the dihedral bond furthest from the hydrocarbon is oriented roughly parallel to the nucleoside's long axis). The γ' value of −94° for the putative minor conformer obtained from molecular mechanics is close to the β' value of −100° obtained by Broyde et al. for the lowest energy domains of the (−)-*cis* adducts of dGuo and dAdo (*72*, *74*).

The observed formation of a cis N-3 BPDE−dCyd adduct raises the question as to why a trans N-3 adduct was not also identified. Possibly, such an adduct did form but escaped identification due to lower stability or yield. In the chromatograms of dCyd and dUrd alkylation products of both BPDE enantiomers, there are additional unidentified small peaks. The cis N-3 adduct may have formed in larger yield because of favorable hydrocarbon−base interactions (which are generally stronger in cis adducts) that compensated for unfavorable steric constraints associated with N-3 alkylation.

This is the first report of the formation of an N-3 adduct of deoxycytidine by a PAH diol epoxide. No such adduct has yet been found in DNA alkylation products; the only dCyd adducts reported thus far have been trans N^4 adducts. In duplex DNA, the N-3 site is part of the central of the three GC base pair hydrogen bonds, which would inhibit access to this site if alkylation proceeded by a collisional mechanism, but might not if the alkylating precursor was intercalated. The N^4 site is in the major

[3] Wolfe, A. R., and Meehan, T. Unpublished data.

groove side of the GC base pair and would be potentially accessible to both external and intercalated BPDE. In the cases of 7-bromomethylbenz[*a*]anthracene and its 12-methyl derivative, DNA denaturation had little effect on the amount of N^4-dCyd product formed, while it decreased the formation of the N^2-dGuo product and increased the formation of the N^6-dAdo product (*75*).

Modified base pair disruption is not inevitable when the exocyclic amino groups of dGuo or dAdo (residing in the minor and major grooves, respectively) are alkylated by an agent even as bulky as BPDE (*76*, *77*). In the case of BPDE-N^2-dGuo adducts, the base pair is disrupted if the adduct intercalates (entering from the minor groove side) but not if it resides in the minor groove. BPDE-N^6-dAdo adducts can intercalate (entering from the major groove side) without disrupting the modified base pair. If the groove environment of the alkylation site is an important determinant of these behaviors, an outcome similar to that for dAdo adducts might be expected for BPDE-N^4-dCyd adducts. In contrast, alkylation at N-3 of dCyd would unavoidably disrupt the affected base pair. Work using BPDE−dGuo adducts has shown that human nucleotide excision repair enzymes preferentially target base pair-disrupting adducts (*78*). While the mutagenic properties of N-3 dCyd adducts of ethylene and propylene oxides have been characterized using in vitro and bacterial systems (*46*, *47*), such studies have yet to be carried out on PAH−dCyd adducts.

Acknowledgment. This work was supported in part by grants from the NIH (CA 40598, ES06869, and AI39152) and the California State Toxic Substances Research and Teaching Program. We thank Dr. Vladimir Basus for assistance in obtaining NMR spectra and Prof. George Negrete for helpful discussions. Mass spectrometry was carried out at the UCSF Mass Spectrometry Facility, an NIH-supported National Research Resource. Tritium-labeled *anti*-BPDE enantiomers were obtained from the NCI Chemical Carcinogen Reference Standard Repository.

Supporting Information Available: Table S1, yields of dCyd and dCMP adduct formation with (+)- and (−)-*anti*-BPDE; Table S2, UV absorbance and CD spectral data for BPDE−dCyd adducts in methanol; Table S3, UV absorbance and fluorescence data for BPDE adducts of cytidine, 3-methylcytidine, or 2′-O-methylcytidine in methanol; Table S4, NMR data for the acetylated dCyd adducts in acetone-d_6 (major conformer only for NF cis dCyd adduct); Table S5, NMR data for both conformers of the acetylated NF cis dCyd adduct in acetone-d_6; Table S6, NMR data for both conformers of the nonacetylated NF cis dCyd adduct in DMSO-d_6. Figure S1, the effect of bromide ion on BPDE−dCMP adduct yield; Figure S2, CD spectra of the dCyd adducts of (+)-*anti*-BPDE (in methanol); Figure S3, the methine proton region of the 600 MHz ^{1}H NMR spectrum of the peracetylated FL cis dCyd adduct of (−)-*anti*-BPDE after deuterium exchange; Figure S4, the ^{1}H NMR spectra of the aromatic region of the acetylated (−) FL cis dCyd adduct in acetone; Figure S5, the ^{1}H NMR spectra of the aromatic region of the acetylated (−)-trans dCyd adduct in acetone; Figure S6, the ^{1}H NMR spectra of the aromatic region of the acetylated (−) NF cis dCyd adduct in acetone; Figure S7, the two-dimensional NOESY spectrum of the acetylated (−)-*anti*-BPDE NF cis dCyd adduct; Figure S8, the effect of methanol on fluorescence emission of *trans*-BPT and the FL and NF cis dCyd adducts of (−)-*anti*-BPDE; Figures S9 and S10, steric energy vs pyrimidine orientation for the *cis* N-3 uracil adduct of (−)-*anti*-BPDE; Figure S11, steric energy vs deoxyribose orientation for the *cis* N-3 dUrd adduct of (−)-*anti*-BPDE. Steric energy plots of pyrimidine rotations in the N-3 Ura adduct; QuickTime movies (with animated energy plots) of the N-3 Ura adduct conformation during forced rotation of the pyrimidine moiety; models of Ura and dUrd adduct gas phase energy minima in Chem3D, QuickTime, or Protein Data Bank formats; information on implicit solution-phase Ura and dUrd adduct minima; and spreadsheets comparing NMR chemical shifts for various dCyd and dUrd adducts. This material is available free of charge via the Internet at http://pubs.acs.org.

References

(1) Geacintov, N. E., Shahbaz, M., Ibanez, V., Moussaoui, K., and Harvey, R. G. (1988) Base-sequence dependence of noncovalent complex formation and reactivity of benzo[*a*]pyrene diol epoxide with polynucleotides. *Biochemistry 27*, 8380−8387.

(2) Szeliga, J., and Dipple, A. (1998) DNA adduct formation by polycyclic aromatic hydrocarbon dihydrodiol epoxides. *Chem. Res. Toxicol. 11*, 1−11.

(3) Jerina, D. M., Chadha, A., Cheh, A. M., Schurdak, M. E., Wood, A. W., and Sayer, J. M. (1991) Covalent bonding of bay-region diol epoxides to nucleic acids. *Adv. Exp. Med. Biol. 283*, 533−553.

(4) Jernström, B., and Gräslund, A. (1994) Covalent binding of benzo[*a*]pyrene 7,8-dihydrodiol 9,10-epoxides to DNA: molecular structures, induced mutations and biological consequences. *Biophys. Chem. 49*, 185−199.

(5) Cheng, S. C., Hilton, B. D., Roman, J. M., and Dipple, A. (1989) DNA adducts from carcinogenic and noncarcinogenic enantiomers of benzo[*a*]pyrene dihydrodiol epoxide. *Chem. Res. Toxicol. 2*, 334−340.

(6) Chen, L., Devanesan, P. D., Higginbotham, S., Ariese, F., Jankowiak, R., Small, G. J., Rogan, E. G., and Cavalieri, E. L. (1996) Expanded analysis of benzo[*a*]pyrene-DNA adducts formed in vitro and in mouse skin: their significance in tumor initiation. *Chem. Res. Toxicol. 9*, 897−903.

(7) Chen, L., Devanesan, P. D., Byun, J., Gooden, J. K., Gross, M. L., Rogan, E. G., and Cavalieri, E. L. (1997) Synthesis of depurinating DNA adducts formed by one-electron oxidation of 7H-dibenzo[*c*,*g*]carbazole and identification of these adducts after activation with rat liver microsomes. *Chem. Res. Toxicol. 10*, 225−233.

(8) Penning, T. M., Burczynski, M. E., Hung, C. F., McCoull, K. D., Palackal, N. T., and Tsuruda, L. S. (1999) Dihydrodiol dehydrogenases and polycyclic aromatic hydrocarbon activation: generation of reactive and redox active o-quinones. *Chem. Res. Toxicol. 12*, 1−18.

(9) Wolfe, A. R., Yamamoto, J., and Meehan, T. (1994) Chloride ions catalyze the formation of cis adducts in the binding of *anti*-benzo[*a*]pyrene diol epoxide to nucleic acids. *Proc. Natl. Acad. Sci. U.S.A. 91*, 1371−1375.

(10) Wolfe, A. R., and Meehan, T. (1994) Halide-catalyzed cis product formation in the hydrolysis of *anti*-benzo[*a*]pyrene diol epoxide and its alkylation of poly(A). *Chem. Res. Toxicol. 7*, 110−119.

(11) Wolfe, A. R., Song, Q., and Meehan, T. (1996) The effect of temperature on the stereochemistry of DNA adducts derived from benzo[*a*]pyrene diol epoxide in the presence and absence of halide ions. *Polycyclic Aromat. Compd. 10*, 203−210.

(12) Meehan, T., Wolfe, A. R., Negrete, G. R., and Song, Q. (1997) Benzo[*a*]pyrene diol epoxide-DNA cis adduct formation through a trans chlorohydrin intermediate. *Proc. Natl. Acad. Sci. U.S.A. 94*, 1749−1754.

(13) Song, Q., Negrete, G. N., Wolfe, A. R., Wang, K., and Meehan, T. (1998) Synthesis and characterization of bay region halohydrins derived from benzo[*a*]pyrene diol epoxide and their role as intermediates in halide-catalyzed cis adduct formation. *Chem. Res. Toxicol. 11*, 1057−1066.

(14) Vock, E. H., Wolfe, A. R., and Meehan, T. (2001) Trans- and cis-DNA adduct concentration in epidermis from mouse and rat skin treated ex vivo with benzo[*a*]pyrene diol epoxide and its corresponding chlorohydrin. *Mutat. Res. 478*, 199−206.

(15) Foskett, J. K. (1990) $[Ca^{2+}]_i$ modulation of Cl^- content controls cell volume in single salivary acinar cells during fluid secretion. *Am. J. Physiol. 259*, C998−C1004.

(16) Takemura, T., Sato, F., Saga, K., Suzuki, Y., and Sato, K. (1991) Intracellular ion concentrations and cell volume during cholinergic stimulation of eccrine secretory coil cells. *J. Membr. Biol. 119*, 211−219.

(17) Meehan, T., Straub, K., and Calvin, M. (1977) Benzo[*a*]pyrene diol epoxide covalently binds to deoxyguanosine and deoxyadenosine in DNA. *Nature (London) 269*, 725−727.

(18) Straub, K. M., Meehan, T., Burlingame, A. L., and Calvin, M. (1977) Identification of the major adducts formed by reaction of

benzo[*a*]pyrene diol epoxide with DNA in vitro. *Proc. Natl. Acad. Sci. U.S.A. 74*, 5285−5289.

(19) Jennette, K. W., Jeffrey, A. M., Blobstein, S. H., Beland, F. A., Harvey, R. G., and Weinstein, I. B. (1977) Nucleoside Adducts from the in vitro reaction of benzo[*a*]pyrene-7,8-dihydrodiol 9,-10-oxide or benzo[*a*]pyrene 4,5-oxide with nucleic acids. *Biochemistry 16*, 932−938.

(20) Brown, H. S., Jeffrey, A. M., and Weinstein, I. B. (1979) Formation of DNA adducts in 10T1/2 mouse embryo fibroblasts incubated with benzo[*a*]pyrene or dihydrodiol oxide derivatives. *Cancer Res. 39*, 1673−1677.

(21) Sayer, J. M., Chadha, A., Agarwal, S. K., Yeh, H. J. C., Yagi, H., and Jerina, D. M. (1991) Covalent nucleoside adducts of benzo-[*a*]pyrene 7,8-diol 9,10-epoxides: structural reinvestigation and characterization of a novel adenosine adduct on the ribose moiety. *J. Org. Chem. 56*, 20−29.

(22) Yamamoto, J., Subramaniam, R., Wolfe, A. R., and Meehan, T. (1990) The formation of covalent adducts between benzo[*a*]-pyrenediol epoxide and RNA: structural analysis by mass spectrometry. *Biochemistry 29*, 3966−3972.

(23) Chadha, A., Sayer, J. M., Yeh, H. J. C., Yagi, H., Cheh, A. M., Pannell, L. K., and Jerina, D. M. (1989) Structures of covalent nucleoside adducts formed from adenine, guanine, and cytosine bases of DNA and the optically active bay-region 3,4-diol 1,2-epoxides of dibenz[*a*,*j*]anthracene. *J. Am. Chem. Soc. 111*, 5456−5463.

(24) Chadha, A., Sayer, J. M., Agarwal, S. K., Cheh, A. M., Yagi, H., Yeh, H. J. C., and Jerina, D. M. (1991) Formation of covalent adducts between DNA and optically active bay-region diol epoxides of dibenzo[*a*,*j*]anthracene. In *Polynuclear Aromatic Hydrocarbons: Measurements, Means and Metabolism (Eleventh International Symposium)* (Cook, M., Loening, K., and Merritt, J., Eds.) pp 179−193, Battelle Press, Columbus, OH.

(25) Cheh, A. M., Chadha, A., Sayer, J. M., Yeh, H. J. C., Yagi, H., Pannell, L. K., and Jerina, D. M. (1993) Structures of covalent nucleoside adducts formed from adenine, guanine, and cytosine bases of DNA and the optically active bay-region 3,4-diol 1,2-epoxides of benz[*a*]anthracene. *J. Org. Chem. 58*, 4013−4022.

(26) Jerina, D. M., Sayer, J. M., Agarwal, S. K., Yagi, H., Levin, W., Wood, A. W., Conney, A. H., Pruess-Schwartz, D., Baird, W. M., Pigott, M. A., and et al. (1986) Reactivity and tumorigenicity of bay-region diol epoxides derived from polycyclic aromatic hydrocarbons. *Adv. Exp. Med. Biol. 197*, 11−30.

(27) Dipple, A., Pigott, M. A., Agarwal, S. K., Yagi, H., Sayer, J. M., and Jerina, D. M. (1987) Optically active benzo[*c*]phenanthrene diol epoxides bind extensively to adenine in DNA. *Nature 327*, 535−536.

(28) Sage, E., and Haseltine, W. A. (1984) High ratio of alkali-sensitive lesions to total DNA modification induced by benzo[*a*]pyrene diol epoxide. *J. Biol. Chem. 259*, 11098−11102.

(29) Bigger, C. A. H., Cheh, A. M., Dipple, A., Yagi, H., Sayer, J. M., and Jerina, D. M. (1986) Sites of alkali-sensitive DNA lesions induced by enantiomers of the diastereomeric bay-region benzo-[*c*]phenanthrene (B[*c*]Ph) 3,4-diol-1,2-epoxides. *Proc. Am. Assoc. Cancer Res. 27*, 88.

(30) Ramos, L. A., Ponten, I., Dipple, A., Kumar, S., Yagi, H., Sayer, J. M., Kroth, H., Kalena, G., and Jerina, D. M. (2002) Site-specific mutagenesis in *Escherichia coli* by N^2-deoxyguanosine adducts derived from the highly carcinogenic fjord-region benzo[*c*]phenanthrene 3,4-diol 1,2-epoxides. *Chem. Res. Toxicol. 15*, 1619−1626.

(31) Peltonen, K., Cheng, S. C., Hilton, B. D., Lee, H., Cortez, C., Harvey, R. G., and Dipple, A. (1991) Effect of bay region methyl group on reactions of *anti*-benz[*a*]anthracene 3,4-dihydrodiol 1,2-epoxides with DNA. *J. Org. Chem. 56*, 4181−4188.

(32) Wei, S. J., Chang, R. L., Bhachech, N., Cui, X. X., Merkler, K. A., Wong, C. Q., Hennig, E., Yagi, H., Jerina, D. M., and Conney, A. H. (1993) Dose-dependent differences in the profile of mutations induced by (+)-7*R*,8*S*-dihydroxy-9*S*,10*R*-epoxy-7,8,9,10-tetrahydrobenzo[*a*]pyrene in the coding region of the hypoxanthine (guanine) phosphoribosyltransferase gene in Chinese hamster V-79 cells. *Cancer Res. 53*, 3294−3301.

(33) Yagi, H., Akagi, H., Thakker, D. R., Mah, H. D., Koreeda, M., and Jerina, D. M. (1977) Absolute stereochemistry of the highly mutagenic 7,8-diol 9,10-epoxides derived from the potent carcinogen *trans*-7,8-dihydroxy-7,8-dihydrobenzo[*a*]pyrene. *J. Am. Chem. Soc. 99*, 2358−2359.

(34) Moore, P. D., and Koreeda, M. (1976) Application of the change in partition coefficient with pH to the structure determination of alkyl substituted guanosines. *Biochem. Biophys. Res. Commun. 73*, 459−464.

(35) Dudek, M. J., and Ponder, J. W. (1995) Accurate modeling of the intramolecular electrostatic energy of proteins. *J. Comput. Chem. 16*, 791−816.

(36) Stewart, J. J. P. (1989) Optimization of parameters for semiempirical methods I. Method. *J. Comput. Chem. 10*, 210−220.

(37) Stewart, J. J. (1990) MOPAC: a semiempirical molecular orbital program. *J. Comput.-Aided Mol. Des. 4*, 1−105.

(38) Klamt, A., and Shüürmann, G. (1993) COSMO: a new approach to dielectric screening in solvents with explicit expressions for the screening energy and its gradient. *J. Chem. Soc. Perk. Trans. 2*, 799−805.

(39) Jeffrey, A. M., Jennette, K. W., Blobstein, S. H., Weinstein, I. B., Beland, F. A., Harvey, R. G., Kasai, H., Miura, I., and Nakanishi, K. (1976) Benzo[*a*]pyrene-nucleic acid derivative found in vivo: structure of a benzo[*a*]pyrenetetrahydrodiol epoxide-guanosine adduct. *J. Am. Chem. Soc. 98*, 5714−5715.

(40) Jeffrey, A. M., Grzeskowiak, K., Weinstein, I. B., Nakanishi, K., Roller, P., and Harvey, R. G. (1979) Benzo[*a*]pyrene-7,8-dihydrodiol 9,10-oxide adenosine and deoxyadenosine adducts: structure and stereochemistry. *Science 206*, 1309−1311.

(41) Dunn, D. B., and Hall, H. R. (1975) Purines, pyrimidines, nucleosides and nucleotides: physical constants and spectral properties. In *CRC Handbook of Biochemistry and Molecular Biology*, 3rd ed. (Fasman, G. D., Ed.) Vol. 2:1, pp 65−215, CRC Press, Cleveland.

(42) Solomon, J. J., Mukai, F., Fedyk, J., and Segal, A. (1988) Reactions of propylene oxide with 2′-deoxynucleosides and in vitro with calf thymus DNA. *Chem.-Biol. Interact. 67*, 275−294.

(43) Solomon, J. J., and Segal, A. (1989) DNA adducts of propylene oxide and acrylonitrile epoxide: hydrolytic deamination of 3-alkyl-dCyd to 3-alkyl-dUrd. *Environ. Health Perspect. 81*, 19−22.

(44) Solomon, J. J., Singh, U. S., and Segal, A. (1993) In vitro reactions of 2-cyanoethylene oxide with calf thymus DNA. *Chem.-Biol. Interact. 88*, 115−135.

(45) Li, F., Segal, A., and Solomon, J. J. (1992) In vitro reaction of ethylene oxide with DNA and characterization of DNA adducts. *Chem.-Biol. Interact. 83*, 35−54.

(46) Bhanot, O. S., Singh, U. S., and Solomon, J. J. (1994) The role of 3-hydroxyethyldeoxyuridine in mutagenesis by ethylene oxide. *J. Biol. Chem. 269*, 30056−30064.

(47) Snow, E. T., Singh, J., Koenig, K. L., and Solomon, J. J. (1994) Propylene oxide mutagenesis at template cytosine residues. *Environ. Mol. Mutagen. 23*, 274−280.

(48) Singh, U. S., Decker-Samuelian, K., and Solomon, J. J. (1996) Reaction of epichlorohydrin with 2′-deoxynucleosides: characterization of adducts. *Chem.-Biol. Interact. 99*, 109−128.

(49) Selzer, R. R., and Elfarra, A. A. (1997) Chemical modification of deoxycytidine at different sites yields adducts of different stabilities: characterization of N3- and O2-deoxycytidine and N3-deoxyuridine adducts of butadiene monoxide. *Arch. Biochem. Biophys. 343*, 63−72.

(50) Barlow, T., and Dipple, A. (1999) Formation of deaminated products in styrene oxide reactions with deoxycytidine. *Chem. Res. Toxicol. 12*, 883−886.

(51) Koskinen, M., Calebiro, D., and Hemminki, K. (2000) Styrene oxide-induced 2′-deoxycytidine adducts: implications for the mutagenicity of styrene oxide. *Chem.-Biol. Interact. 126*, 201−213.

(52) Segal, A., Solomon, J. J., and Mukai, F. (1990) In vitro reactions of glycidol with pyrimidine bases in calf thymus DNA. *Cancer Biochem. Biophys. 11*, 59−67.

(53) Geacintov, N. E., Mao, B., France, L. L., Zhao, R., Chen, J., Liu, T. M., Ya, N.-Q., Margulis, L. A., and Sutherland, J. C. (1992) Photoinduced electron transfer and fluorescence mechanisms in covalently linked polynuclear aromatic-nucleotide complexes. *SPIE Vol. 1640, Time-Resolved Laser Spectroscopy in Biochemistry III*, 774−783.

(54) Sayer, J. M., Yagi, H., Silverton, J. V., Friedman, S. L., Whalen, D. L., and Jerina, D. M. (1982) Conformational effects in the hydrolyses of rigid benzylic epoxides: implications for diol epoxides of polycyclic hydrocarbons. *J. Am. Chem. Soc. 104*, 1972−1978.

(55) Sayer, J. M., Whalen, D. L., Friedman, S. L., Paik, A., Yagi, H., Vyas, K. P., and Jerina, D. M. (1984) Conformational effects in the hydrolyses of benzo-ring diol epoxides that have bay-region diol groups. *J. Am. Chem. Soc. 106*, 226−233.

(56) Doan, L., Yagi, H., Jerina, D. M., and Whalen, D. L. (2002) Chloride Ion Catalyzed Conformational Inversion of Carbocation Intermediates in the Hydrolysis of a Benzo[*a*]pyrene 7,8-Diol 9,-10-Epoxide. *J. Am. Chem. Soc. 124*, 14382−14387.

(57) Singer, B. (1975) The chemical effects of nucleic acid alkylation and their relation to mutagenesis and carcinogenesis. *Prog. Nucleic Acid Res. Mol. Biol. 15*, 219−284.

(58) Singer, B. (1986) O-alkyl pyrimidines in mutagenesis and carcinogenesis: occurrence and significance. *Cancer Res. 46*, 4879−4885.
(59) Sun, L., and Singer, B. (1974) Reaction of cytidine with ethylating agents. *Biochemistry 13*, 1905−1913.
(60) Dipple, A., Brookes, P., Mackintosh, D. S., and Rayman, M. P. (1971) Reaction of 7-bromomethylbenz[*a*]anthracene with nucleic acids, polynucleotides, and nucleosides. *Biochemistry 10*, 4323−4330.
(61) Shapiro, R., and Shiuey, S.-J. (1976) Reactions of cytidine with 7-bromomethylbenz[*a*]anthracene, benzyl bromide, and *p*-methoxybenzyl bromide. Ratio of amino to 3 substitution. *J. Org. Chem. 41*, 1597−1600.
(62) Dipple, A. (1995) DNA adducts of chemical carcinogens. *Carcinogenesis (London) 16*, 437−441.
(63) Singer, B., Kröger, M., and Carrano, M. (1978) O^2- and O^4-alkyl pyrimidine nucleosides: stability of the glycosyl bond and of the alkyl group as a function of pH. *Biochemistry 17*, 1246−1250.
(64) Singer, B. (1976) O^2-alkylcytidine—a new major product of neutral, aqueous reaction of cytidine with carcinogens. *FEBS Lett. 63*, 85−88.
(65) Koreeda, M., Moore, P. D., Yagi, H., Yeh, H. J., and Jerina, D. M. (1976) Alkylation of polyguanylic acid at the 2-amino group and phosphate by the potent mutagen (±)-7β,8α-dihydroxy-9β,10β-epoxy-7,8,9,10-tetrahydrobenzo[*a*]pyrene. *J. Am. Chem. Soc. 98*, 6720−6722.
(66) Geacintov, N. E., Cosman, M., Mao, B., Alfano, A., Ibanez, V., and Harvey, R. G. (1991) Spectroscopic characteristics and site I/site II classification of cis and trans benzo[*a*]pyrene diolepoxide enantiomer-guanosine adducts in oligonucleotides and polynucleotides. *Carcinogenesis (London) 12*, 2099−2108.
(67) Meehan, T., Gamper, H., and Becker, J. F. (1982) Characterization of reversible, physical binding of benzo[*a*]pyrene derivatives to DNA. *J. Biol. Chem. 257*, 10479−10485.
(68) Geacintov, N. E., Yoshida, H., Ibanez, V., and Harvey, R. G. (1982) Noncovalent binding of 7β,8α-dihydroxy-9α,10α-epoxytetrahydrobenzo[*a*]pyrene to deoxyribonucleic acid and its catalytic effect on the hydrolysis of the diol epoxide to tetrol. *Biochemistry 21*, 1864−1869.
(69) Geacintov, N. E., Zhao, R., Kuzmin, V. A., Kim, S. K., and Pecora, L. J. (1993) Mechanisms of quenching of the fluorescence of a benzo[*a*]pyrene tetraol metabolite model compound by 2′-deoxynucleosides. *Photochem. Photobiol. 58*, 185−194.
(70) Shafirovich, V. Y., Levin, P. P., Kuzmin, V. A., Thorgeirsson, T. E., Kliger, D. S., and Geacintov, N. E. (1994) Photoinduced electron transfer and enhanced triplet yields in benzo[*a*]pyrene derivative-nucleic acid complexes and covalent adducts. *J. Am. Chem. Soc. 116*, 63−72.
(71) Xie, X. M., Geacintov, N. E., and Broyde, S. (1999) Stereochemical origin of opposite orientations in DNA adducts derived from enantiomeric anti-benzo[*a*]pyrene diol epoxides with different tumorigenic potentials. *Biochemistry 38*, 2956−2968.
(72) Xie, X. M., Geacintov, N. E., and Broyde, S. (1999) Origins of conformational differences between cis and trans DNA adducts derived from enantiomeric anti-benzo[*a*]pyrene diol epoxides. *Chem. Res. Toxicol. 12*, 597−609.
(73) Tan, J., Geacintov, N. E., and Broyde, S. (2000) Principles governing conformations in stereoisomeric adducts of bay region benzo[*a*]pyrene diol epoxides to adenine in DNA: steric and hydrophobic effects are dominant. *J. Am. Chem. Soc. 122*, 3021−3032.
(74) Tan, J., Geacintov, N. E., and Broyde, S. (2000) Conformational determinants of structures in stereoisomeric cis-opened anti-benzo[*a*]pyrene diol epoxide adducts to adenine in DNA. *Chem. Res. Toxicol. 13*, 811−822.
(75) Rayman, M. P., and Dipple, A. (1973) Structure and activity in chemical carcinogenesis. Comparison of the reactions of 7-bromomethylbenz[*a*]anthracene and 7-bromomethyl-12-methylbenz[*a*]anthracene with deoxyribonucleic acid in vitro. *Biochemistry 12*, 1202−1207.
(76) Geacintov, N. E., Cosman, M., Hingerty, B. E., Amin, S., Broyde, S., and Patel, D. J. (1997) NMR solution structures of stereoisometric covalent polycyclic aromatic carcinogen-DNA adduct: principles, patterns, and diversity. *Chem. Res. Toxicol. 10*, 111−146.
(77) Mao, B., Gu, Z., Gorin, A., Chen, J., Hingerty, B. E., Amin, S., Broyde, S., Geacintov, N. E., and Patel, D. J. (1999) Solution structure of the (+)-cis-anti-benzo[*a*]pyrene-dA ([BP]dA) adduct opposite dT in a DNA duplex. *Biochemistry 38*, 10831−10842.
(78) Hess, M. T., Gunz, D., Luneva, N., Geacintov, N. E., and Naegeli, H. (1997) Base pair conformation-dependent excision of benzo[*a*]pyrene diol epoxide-guanine adducts by human nucleotide excision repair enzymes. *Mol. Cell. Biol. 17*, 7069−7076.

TX0340201